Incorporation of Recombinant Fibronectin Into Genetically Engineered Elastin-based Polymers

A Thesis
Presented to
The Academic Faculty

by

Fanor Alberto Balderrama

In Partial Fulfillment
of the Requirements for the Degree
Master of Science in the
School of Bioengineering

Georgia Institute of Technology
December 2009

Incorporation of Recombinant Fibronectin Into Genetically Engineered Elastin-based Polymers

Approved by:

Dr. Elliot L. Chaikof, Advisor
School of Biomedical Engineering
Georgia Institute of Technology
Department of Surgery
Emory University School of Medicine

Dr. Hanjoong Jo
School of Biomedical Engineering
Georgia Institute of Technology
Division of Cardiology
Emory University School of Medicine

Dr. Vincent P. Conticello
School of Chemistry
Emory University

Date Approved: November 11, 2009

ACKNOWLEDGEMENTS

I would like to thank my advisor, Dr. Elliot Chaikof, for the opportunity of working on this research and for all the guidance. I would also like to thank Dr. Carolyn Haller for all her priceless guidance, her supervision and patience, without which this thesis would have not been possible.

My sincere appreciation goes out to members of my committee: Dr. Hanjoong Jo and Dr. Vincent Conticello for their help with the direction and the review of this thesis.

I would also like to thank all the other members of the Chaikof laboratory for their friendship, their help and their advice, without which my research experience would have not been so enjoyable.

Last, but absolutely not least, I thank my family for all their support (professional, emotional and even financial) and their faith in me.

TABLE OF CONTENTS

LIST OF FIGURES

LIST OF ABBREVIATIONS

BBP	BSA-blocked polystyrene
BSA	Bovine serum albumin
CVD	Cardiovascular disease
ECM	Extracellular matrix
EDC	1-ethyl-3-[3-dimethylaminopropyl] carbodiimide
ePTFE	Expanded polytetrafluoroethylene
GPX	Genipin-crosslinked $FNIII_{7-10}$ onto LysB10 hydrogels
hpFN	Human plasma fibronectin
HRP	Horseradish peroxidase
HUVEC	Human umbilical vascular endothelial cell
IPTG	Isopropyl beta-D-1-thiogalactopyranoside
NGF	Nerve growth factor
PAG	Passively adsorbed rFN onto LysB10 hydrogels
PBS	Phosphate buffer solution
PEI	Poly(ethyleneimine)
PET	Polyethylene terephthalate

PFA	Paraformaldehyde
PHSRN	Proline-histidine-serine-arginine-asparagine
POD	Peroxidase
PTFE	Polytetrafluoroethylene
PU	Polyurethane
rFN	Recombinant fibronectin ($FNIII_{7-10}$)
RGD	Arginine-glycine-aspartic acid peptide sequence
SDS-PAGE	Sodium dodecyl sulfate polyacrylamide gel electrophoresis
Strep-AP	Streptavidin-alkaline phosphatase conjugate
Sulfo-SMCC	Sulfosuccinimidyl 4-[N-maleimidomethyl] cyclohexane-1-carboxylate
UTG	Untreated LysB10 hydrogels

SUMMARY

This thesis describes a new complex biomaterial that combines recombinant elastin and fibronectin proteins in a covalently crosslinked hydrogel. This material is intended to be applied in vascular grafts, and it is with this objective in mind that the two proteins were chosen. Elastin, along with collagen plays an important role in the mechanical properties of vasculature. Fibronectin has been extensively studied for its cell-binding properties and its ability to promote tissue integration when incorporated on biomaterials. The resulting material consists on a porous elastin-mimetic hydrogel presenting the cell-binding domains of fibronectin.

First, it was assessed that recombinant fibronectin (rFN) preserves similar cell binding capabilities of human plasma fibronectin through cell adhesion assays where human umbilical vein endothelial cells (HUVECs) were used. Furthermore, it was observed that when coating inert surfaces, greater concentrations of rFN resulted in greater numbers of cells adhered to these surfaces, indicating that rFN was responsible for the increase in cell adhesion. By means of these adhesion tests, it was also observed that elastin mimetic hydrogels without rFN did not support significant levels of cell adhesion. Recombinant fibronectin was chemically crosslinked and incorporated onto elastin mimetic hydrogels, and the modified substrates supported cell adhesion and proliferation. Furthermore, the stability of the crosslinking incorporation was verified.

CHAPTER I

INTRODUCTION

Cardiovascular disease is the main cause of death in the United States. Many of these conditions require the grafting or bypassing of compromised blood vessels. To this effect, biological vascular grafts, those obtained from the same patient (autologous) or from a member of the same species (allogeneic), are the first line of action. However, when the patient lacks vasculature suitable for grafting use, several synthetic grafting options are available.

The search for an inert biomaterial for vascular grafts has proven to be unsuccessful. This makes the interactions taking place on the blood-biomaterial interface critical for the success of the grafts. While synthetic polymers are the most common group of materials for the fabrication of vascular grafts, several biosynthetic materials have been developed. This thesis introduces a new bio-inspired approach to tackle the mechanical and biological challenges of vascular material design.

The hypothesis of this research is that recombinant fibronectin protein can be stably incorporated onto elastin-mimetic polymers to increase endothelialization. A recombinant version of elastin, designed to recreate the mechanical properties of natural elastin, was used for the preparation of hydrogel surfaces. These surfaces showed low levels of endothelial cell adhesion. For immobilization of recombinant fibronectin, genipin, a chemical crosslinker, was used to covalently link the protein to the elastin-mimetic material. The crosslinked surfaces showed high levels of cell adhesion, and unlike unmodified surfaces simply coated with fibronectin, this biological effect was stable.

Specific Aims and Central Hypothesis

The central hypothesis in this study states that recombinant fibronectin can be used to functionalize elastin mimetic protein substrates for improving endothelialization. This ***Central Hypothesis*** was investigated by pursuing the following specific aims.

The goal of **specific aim 1** was to synthesize recombinant fibronectin and characterize its biological activity on an elastic mimetic surface. We hypothesized that the cell-adhesive activity of our fibronectin protein variant is comparable to natural fibronectin. It was proved that coating inert surfaces with both proteins increased their cell-adhesion levels in a similar manner. Based on that hypothesis, we later proved a second hypothesis for this specific aim, that recombinant fibronectin promotes endothelialization on elastic mimetic surfaces.

The goal of **specific aim 2** was to achieve a stable incorporation of recombinant fibronectin onto the elastic mimetic surfaces. Based on the sequences of both proteins, it was hypothesized that elastin surfaces could be covalently modified with recombinant fibronectin. This objective was achieved with the use of genipin for the crosslinking of both fibronectin and elastin recombinant proteins. It was also hypothesized that by crosslinking our fibronectin protein variant, its cell-adhesive effects would be retained on elastin mimetic substrates. After long incubation, chemically modified surfaces retained the same cell-adhesive activity, while this activity was largely lost on coated elastin mimetic surfaces over the same period of time.

CHAPTER II

LITERATURE REVIEW

According to the American Heart Association Heart Disease and Stroke Statistics-2009 Updates, cardiovascular disease (CVD) imposes an extraordinary socioeconomic cost in the United States. CVD is currently the leading cause of death among Americans, accounting for approximately 35.3 percent of all deaths in the US (1 in every 2.8 deaths), and in 2008 had an associated cost of $475.3 billion. Coronary heart disease (CHD) accounts for 52% of all CVD-related deaths. In 2006 alone, roughly 440,000 cardiac bypass surgery procedures were performed in 253,000 patients in the US [1, 2].

2.1. Biological Grafts

2.1.1. Autografts

It is estimated that 1.4 million patients in the US present arterial tissue deficiencies [3, 4]. Autologous grafts (autografts) are currently the method of choice for vascular replacements in both coronary bypass and peripheral grafting surgeries, generally performing better than synthetic alternatives [5-7]. Patency rates, the likelihood a vascular grafts will remain unblocked, is the most common criteria used to describe the degree of success of grafts. By these terms, autografts have been reliable in cases where they can be applied. The use of the gastropiploic artery for coronary

bypass has been reported to yield 1-, 3- and 5- year patency rates of 98.7, 91.1 and 84.4%, respectively. In similar applications, the same patency rates for the usage of the left internal mammary artery are estimated at 99.6%, 98.8 % and 97.0 % [8]. Other common and successful arteries and veins used for autografts include the radial artery, the saphenous vein, the internal jugular vein and the ipsilateral great saphenous vein, with arterial autografts being usually more successful (in terms of patency rates) than venous grafts [5]. In general, the limitations of autografts are associated with tissue availability. Not every healthy vessel is suitable for use as grafts, and the use of different arteries and veins has met different rates of success, depending also on the site of application. In general, grafting success rate decreases as vasculature decreases in diameter. The length and nature of the lesion can further limit the grafting options. Depending on the procedure, up to 30% of patients do not have vasculature suitable for an autograft due to venous abnormality, poor quality or lack of vessels due to a previous surgery [7].

2.1.2. Allografts

When autografts are not an option, allogeneic transplantation is the most common second line of action. The use of these grafts, however, presents its own challenges. In order to reduce the risk of viral disease transmission from allografts, these are frozen and cryopreserved for several months. The cryopreservation process has been linked to mechanical rupture and aneurysm formation in the grafts in the short term after transplantation, from a few hours to 1 month [9]. Early allografts, especially for peripheral arterial bypass showed mixed rates of success, as measured by patency rate [10, 11]. Failure was attributed to immune reactions. Allograft tanning with

glutaraldehyde has proved to be a useful way of increasing tensile strength and flexibility, masking histocompatibility antigen sites and reducing the risk of allograft biodegradation [12]. It has been suggested, however, that glutaraldehyde leaching can cause delayed biodegradation (due to the loss of crosslinking sites), cytotoxic effects on fibroblasts and foreign body giant cell response [13]. Despite the major improvements from tanning, the 5-year patency rate of these grafts drops in comparison to autografts, down to 67% [5].

2.2. Synthetic Polymer Grafts

Synthetic substitutes have evolved to imitate many of the functions and characteristics of natural tissue. The ideal vascular graft, as defined by Kannan, must be nonthrombogenic, compatible at high blood flow rates, and have similar viscoelasticity to native vessels [14]. The search for a non-reactive biomaterial has proven to be unsuccessful. Biomaterial research has focused on optimizing the interaction with tissue to elicit a controlled reaction and desirable results [15]. The efficacy of these materials in grafts is determined by the blood-biomaterial interface and the mechanical profile match between native vasculature and the biomaterial [16]. Synthetic materials currently employed in vascular grafts include expanded Polytetrafluoroethylene (ePTFE), Dacron ® (DuPont, DE, USA) and polyurethanes (PUs) [14].

2.2.1. Expanded Polytetrafluoroethylene

The high crystallinity and hydrophobicity of ePTFE make it a logical choice for a biomaterial. These properties have important implications in predicting the interactions between the surface of the biomaterial and blood. Its hydrophobicity prevents hydrolysis of the polymer chains and biodegradation of the material within the body. Its electronegativity minimizes its interaction of the material surface with blood [15]. It presents a microporous structure, which is more suitable for cell adhesion and tissue integration than the non-expanded form of polytetrafluoroethylene (PTFE) [14]. ePTFE grafts have greater success when used on large diameter vessels. They perform with a 5-year patency rate of 91% when used as aortic bifurcation grafts [17], but the patency rate drops down to 45% when they are employed for above-knee femoropopliteal bypass [18]. In comparison, autografts perform with a patency rate of 77% in the latter situation [15].

2.2.2 Polyethylene Terephthalate

Polyethylene terephthalate (PET) or Dacron ®, as it was introduced by DuPont in 1939 is a synthetic polymer implemented as either knitted or interwoven multifilament fibers for the making of vascular graft. The porosity of PET grafts is such that the material needs to be preclotted (a process that has been performed with collagen, gelatin and albumin in commercially available grafts) to prevent transmural blood extravasation [14, 19]. Similar to ePTFE, PET possesses a highly crystalline structure and hydrophobic properties [15]. PET aortic bifurcation grafts perform with a 5-year

patency rate of 93% [20]. Comparably to PTFE grafts, however, the 5-year patency rate drops down to 43% on above-knee bypass grafts [18].

2.3. Biopolymers

2.3.1 Collagen

An elegant alternative to synthetic polymers for vascular grafts is the use of ECM proteins that make up part of the native architecture of blood vessels [21]. One of the most studied ECM proteins for this application is Type I Collagen. Type I Collagen is an attractive material for vascular grafts due to its resistance to rupture [22] and critical contribution to the overall elastic modulus of native vasculature, especially at high pressures [23]. Natural collagen also shows potential for endothelialization applications. Davis and Camarillo reported that upon been seeded on Type I collagen gels, human endothelial cells formed capillary networks. This process was dependent on alpha-2-beta-1 integrin cell surface receptors [24, 25], and has, since then, been mapped to a specific integrin-binding amino acid sequence in collagen [26].

Several approaches have been taken to improve mechanical strength of collagen constructs and avoid degradation [5, 21], necessary steps to make them suitable for vascular grafts. These approaches include glutaraldehyde crosslinking [27] (though the risks associated with leaching are still a concern [21]) and mechanical conditioning [28].

2.3.2. Elastin and LysB10

2.3.2.1. Mechanical Importance of Elastin in Vascular Tissue

Elastin and collagen are key structural proteins in the extracellular matrix of vasculature [29], and the mechanical properties of vascular tissue can be attributed to these two proteins and to smooth muscle cells [23, 30]. Collagen provides the tissue the stiffness necessary to withstand blood pressure and limit deformation during excessive strain [30, 31]. Smooth muscle acts as a force-generating component in vasculature under physiological regulation [23, 32]. Elastin provides vasculature with compliance and resilience (distensibility and elastic recovery) necessary to absorb the hemodynamic stress during cardiac systole and release the energy in the form of sustained blood pressure during diastole [33].

The interplay of elastin and collagen proteins defines to a great extent the mechanical properties of blood vessels and their critical importance for circulation. Compliance influences pulse pressure. Ultimately, the limits of organ perfusion are set by the pressure-dependent caliber of blood vessels at full dilation [34] .

2.3.2.2. Structure of Elastin and LysB10

Given the importance of elastin, this protein is a natural choice for a bio-inspired vascular material. Human elastin is synthesized as a 72 kDa soluble precursor, tropoelastin. Tropoelastin, though varying between species and tissue location, generally presents an extremely apolar structure. It is rich in glycine (30-33%), valine (15-18%), proline (10-13%) and other hydrophobic residues (28%) [35, 36]. Recombinant materials allow for a fine tuning of macroscopic characteristics by accessing diverse morphologies [37, 38]. Urry and colleagues, for instance, explored the changes in temperature-dependent behavior brought about by the substitution of a single residue in a basic repeat unit in an elastin-mimetic protein (poly (Val-Pro-Gly-Val-Gly)) where the amino acid in the fourth position is substituted). They observed that the temperature of reversible self-aggregation could change ranging from 5°C to 40°C

depending of the hydrophobicity of the amino acid and the frequency of the substitution [39]. Unlike other proteins, which undergo denaturation and loss of function, elastin and its recombinant variants respond to an increase in temperature by undergoing reversible self-aggregation and forming insoluble fibrillar networks [40], a phenomenon known as coacervation [39].

Our group has developed a new type of elastin-mimetic protein named LysB10. Morphologically, the protein is a multiblock polymer comprised of two hydrophobic blocks flanking and a central hydrophilic block [35]. This molecular arrangement allows for the formation of self-assembled networks [38]. The self-aggregating hydrophobic blocks (predominantly Ile-Pro-Ala-Val-Gly repeats) display plastic-like mechanical properties. These blocks flank a central block that is elastomeric in mechanical nature (Val-Pro-Gly-Xaa-Gly, where Xaa is Ala- or Glu- in a 4:1 ratio) [38, 41] (Figure 2-1). At physiologically relevant conditions (pH ~7.4 and 37 C), the multiblock polymer is present in coacervated form. Physical or non-covalent crosslinks are formed from the aggregation of hydrophobic blocks and the self-association of chemically similar domains [41, 42].

In elastin and elastin-mimetic proteins, the hydrophobic blocks are responsible for self-aggregation and tensile properties. In contrast, the hydrophilic or crosslinking blocks, take part in covalent zero-length crosslinking [43]. Elastin, as found in tissue, is in a crosslinked form. Rapidly after tropoelastin is secreted into the extracellular space, it becomes insoluble. The enzyme lysyl oxydase catalyzes an oxidative deamination of lysine residues in tropoelastin *in vivo* to produce allysine residues [44]. Next, closely positioned lysine and allysine residues from adjacent tropoelastin chains undergo spontaneous condensation to produce covalent crosslinks such as allysine aldol, lysinonorleucine, merodesmosine, and tetrafunctional crosslinks desmosine and

isodesmosine [44-46]. To account for the chemical crosslinking in elastin, small lysine-carrying inserts were introduced between the hydrophobic and hydrophilic blocks in the primary sequence of LysB10 [35] (Figure 2-1). In this study, these lysine groups were targeted for crosslinking. Genipin was used to react with the amine groups on the side chains of the lysine residues and crosslink LysB10 hydrogels and $FNIII_{7-10}$.

Val	**Pro**	**Ala**	**Val**	**Gly**	**Lys**	**Val**	**Pro**	**Ala**	**Val**	**Gly**	**Ile**	**Pro**	**Ala**	**Val**	**Gly**	**Ile**
GTT	CCA	GCT	GTT	GGT	AAG	GTT	CCA	GCG	GTT	GGT	ATC	CCA	GCC	GTG	GGT	ATC
Pro	**Ala**	**Val**	**Gly**	**Ile**	**Pro**	**Ala**	**Val**	**Gly**	**Val**	**Pro**	**Ala**	**Val**	**Gly**	**[Ile**	**Pro**	**Ala**
CCA	GCG	GTT	GGC	ATT	CCG	GCC	GTA	GGC	GTA	CCG	GCG	GTT	GGT	[ATT	CCA	GCG
Val	**Gly**	**Ile**	**Pro**	**Ala**	**Val**	**Gly**	**Ile**	**Pro**	**Ala**	**Val**	**Gly**	**Ile**	**Pro**	**Ala**	**Val**	**Gly**
GTT	GGT	ATC	CCG	GCC	GTG	GGT	ATC	CCA	GCG	GTT	GGC	ATT	CCG	GCC	GTG	GGC
Val	**Pro**	**Ala**	**Val**	**Gly]$_{33}$**	**Ile**	**Pro**	**Ala**	**Val**	**Gly**	**Lys**	**Ala**	**Ala**	**Lys**	**Ala**	**Pro**	**Gly**
GTA	CCG	GCG	GTT	GGT]$_{33}$	ATT	CCA	GCT	GTT	GGT	AAG	GCG	GCC	AAG	GTT	CCA	GGT
Ala	**Gly**	**[Val**	**Pro**	**Gly**	**Ala**	**Gly**	**Val**	**Pro**	**Gly**	**Ala**	**Gly**	**Val**	**Pro**	**Gly**	**Glu**	**Gly**
GCA	GGC	[GTT	CCA	GGT	GCA	GGC	GTA	CCG	GGT	GCT	GGC	GTT	CCG	GGT	GAA	GGT
Val	**Pro**	**Gly**	**Val**	**Gly**	**Val**	**Pro**	**Gly**	**Val**	**Gly]$_{28}$**	**Val**	**Pro**	**Ala**	**Val**	**Gly**	**Lys**	**Ala**
GTT	CCA	GGC	GCA	GGT	GTA	CCG	GGT	GCG	GGT]$_{28}$	GTT	CCA	GCT	GTT	GGT	AAG	GCG
Ala	**Lys**	**Val**	**Pro**	**Gly**	**Ala**	**Gly**	**Val**	**Pro**	**Ala**	**Val**	**Gly**	**Ile**	**Pro**	**Ala**	**Val**	**Gly**
GCC	AAG	GTT	CCA	GGT	GCA	GGC	GTT	CCA	GCT	GTT	GGT	ATC	CCA	GCT	GTT	GGT
Ile	**Pro**	**Ala**	**Val**	**Gly**	**Ile**	**Pro**	**Ala**	**Val**	**Gly**	**Ile**	**Pro**	**Ala**	**Val**	**Gly**	**[Ile**	**Pro**
ATC	CCA	GCT	GTT	GGC	ATT	CCG	GCT	GTA	GGT	ATC	CCG	GCA	GTG	GGC	[ATT	CCG
Ala	**Val**	**Gly**	**Ile**	**Pro**	**Ala**	**Val**	**Gly**	**Ile**	**Pro**	**Ala**	**Val**	**Gly**	**Ile**	**Pro**	**Ala**	**Val**
GCT	GTT	GGT	ATC	CCA	GCT	GTT	GGT	ATC	CCA	GCT	GTT	GGC	ATT	CCG	GCT	GTA
Gly	**Ile**	**Pro**	**Ala**	**Val**	**Gly]$_{33}$**	**Ile**	**Pro**	**Ala**	**Val**	**Gly**	**Lys**	**Ala**	**Ala**	**Lys**	**Ala**	**Stop**
GGT	ATC	CCG	GCA	GTG	GGC]$_{33}$	ATT	CCA	GCT	GTT	GGT	AAG	GCG	GCC	AAG	GCG	TAA

Figure 2-1. Nucleotide and amino acid sequence of LysB10.The plastic and elastic blocks are highlighted in gray and blue, respectively.

2.4 Fibronectin and $FNIII_{7-10}$ (rFN)

Endothelialization is critical for the success of non-biological vascular grafts. Herring and Mansfield suggested that endothelialization would provide a more biocompatible surface and thereby decrease thrombosis and intimal hyperplasia [7, 47, 48]. It has been shown since then that cell-seeded grafts develop an extensive endothelial lining after implantation [49]. In a randomized clinical study, Deutsch and colleges report a primary 9-year patency rate of 68% for ePTFE grafts seeded with autologous endothelial cells and a rate of 16% for unseeded ePTFE grafts (both groups of patients received above-the-knee and bellow-the-knee graftings) [50]. Thrombosis, patency loss, intimal hyperplasia, and ultimately stenosis have hindered the success of synthetic materials *in vivo*, especially when used on small diameter vasculature (> 5mm) [51]. These processes, however, can be reduced by endothelializing the graft lumen, thereby, decreasing protein deposition and infection [49, 51]. Low endothelial cell seeding on synthetic polymeric surfaces, such as ePTFE or Dacron ®, does not suffice for *in vivo* applications. High cell densities are necessary before any implantation as pulsatile flow can detach up to 70% of the seeded cells within 45 minutes after exposure [51, 52]. Hence, improving cell adhesion, retention and proliferation in synthetic and other type of materials is a very active field of vascular tissue engineering research.

Some of the approaches used to increase endothelialization include mechanical [28] or electrostatic pre-conditioning of synthetic materials [53]. The tissue engineering approach postulated in this thesis, however, involves the incorporation of specific biological adhesion cues onto our basal elastin mimetic material. The adhesion cue chosen for our studies is $FNIII_{7-10}$, a recombinant form of fibronectin developed by the

Erickson group [54]. Fibronectin is a well studied glycoprotein of the extracellular matrix (ECM), and it is found in connective tissue throughout the body in humans and in blood plasma [55, 56]. Fibronectin is also expressed as a membrane glycoprotein in some cells, and fibronectin-like domains are found in large glycoprotein complexes in the ECM, such as tenascin [57]. Fibronectin can be found in monomeric and dimeric forms ranging in size from 146,000 to 450,000 Da. Being a major extracellular connective tissue component, fibronectin is distributed extensively on basement membranes [54].

The importance of fibronectin for cell adhesion is illustrated in seminal work that identified fibronectin as a single serum component required for fibroblasts to adhere to collagen substrates *in vitro* and display the morphological changes associated with cell adhesion (flattening and spreading) [58]. $FNIII_{7\text{-}10}$ (hereafter referred to as rFN), was designed after the type III domains 7 through 10 of fibronectin [54, 56, 59]. Of special importance within these domains are two cell-binding amino acid sequences, Arg-Gly-Asp (RGD) and Pro-His-Ser-Arg-Asn (PHSRN), located in the tenth and ninth domain, respectively [60, 61] (Figure 2-2).

RGD is one of the best understood recognition sites in cell adhesion. This ubiquitous tripeptide sequence has been found in fibronectin, vitronectin, type I collagen, von Willebrand factor, osteopontin and in platelet adhesion proteins, among others, where it plays a critical role in cell adhesion and migration [62]. RGD containing peptides have been coated onto synthetic surfaces, resulting in the promoting of fibronectin-like cell adhesion onto otherwise cell-inhospitable substrates [63-65]. Furthermore, RGD-containing peptides in solution are capable of blocking cell adhesion by binding and occupying the RGD recognition sites on cell membrane receptors. Even the smallest alterations in the tripeptide sequence, such as replacing alanine for glycine

residue or aspartic acid for the glutamic acid residue, can eliminate these cell binding phenomena [66].

The role of PHSRN, on the other hand, is only complementary, i.e. synergistic only, to RGD. In competitive binding assays, peptides containing RGD and PSHRN in solution blocked cell binding to fibronectin-coated surfaces better than peptides containing only RGD, while peptides containing only PHSRN did not show significant inhibitory activity [60]. Petrie and Garcia suggest that PHSRN may play a role in the integrin binding specificity. They report that both RGD and PHSRN sites, and only in the same spatial context within the type III domains of fibronectin, are necessary for specific binding to alpha-5-beta-1 integrin cell receptors. Other synthetic peptides presenting RGD only, and even RGD and PHSRN sites combined, promote binding to alpha-v-beta-3 integrins, instead [61].

Biotin binding domain

M K L K V T V N G T A Y D V D V D V D K S H E N P M G T I L F G
G G T G G A P A P A A G G A G A G K A G E G E I P A P L A G T V
S K I L V K E G D T V K A G Q T V L V L E A M K M E T E I N A P
T D G K V E K V L V K E R D A V Q G G Q G L I K I G D L E L I E
G R E K L M

FNIII$_7$ domain

P L S P P T N L H L E A N P D T G V L T V S W E R S T T P D I T
G Y R I T T T P T N G Q Q G N S L E E V V H A D Q S S C T F D N
L S P G L E Y N V S V Y T V K D D K E S V P I S D T I I P

FNIII$_8$ domain

A V P P P T D L R F T N I G P D T M R V T W A P P P S I D L T N
F L V R Y S P V K N E E D V A E L S I S P S D N A V V L T N L L
P G T E Y V V S V S S V Y E Q H E S T P L R G R Q K T

FNIII$_9$ domain

G L D S P T G I D F S D I T A N S F T V H W I A P R A T I T G Y
R I R H H P E H F S G R P R E D R V P H S R N S I T L T N L T P
G T E Y V V S I V A L N G R E E S P L L I G Q Q S T

FNIII$_{10}$ domain

V S D V P R D L E V V A A T P T S L L I S W D A P A V T V R Y Y
R I T Y G E T G G N S P V Q E F T V P G S K S T A T I S G L K P
G V D Y T I T V Y A V T G R G D S P A S S K P I S I N Y R T

Figure 2-2. Amino acid sequence of rFN organized by domains. RGD and PHSRN binding sites are highlighted in blue and gray, respectively.

2.5. Integrins and Focal Adhesions

Integrins are the most important cell receptors for the extracellular matrix. Integrins are also signal transduction receptors, relaying information about adhesive ligands to control cell growth and structure [67]. Their name denotes the role they play linking the ECM and the cytoskeleton, though integrins regulate many more aspects of cell behavior other than cytoskeleton [68]. Fibronectin binds to at least nine different integrins. Both laminin and von Willebrand's factor bind to at least five different integrins. This promiscuity may reflect common motifs, such as RGD, in otherwise unrelated ligands [67].

Structurally, integrins are heterodimers of one of 18 alpha subunits and one of 8 beta subunits [68], both having large extracellular segments and short transmembrane and cytoplasmic segments [69]. Both subunits contribute to binding specificity, which allows for a combinatorial strategy to establish an integrin repertoire [67]. In this manner, alpha-2-beta-1 integrins binds to Type-I collagen [70] and to certain fibronectin species, though not by RGD binding. Alpha-v-beta-3 integrins bind to fibrinogen and fibronectin through RGD sequences in the ECM proteins [67, 71]. Of special importance for this study is the observation by Petrie and colleagues that rFN binds to fibroblasts primarily by alpha-5-beta-1 integrins with great specificity through RGD and PHSRN sequences [61], and the demonstration by Dormond et al. that the same integrins are present in HUVEC and constitute the principal receptor involved in the binding of HUVEC to fibronectin [72].

Fibronectin binding to integrin is followed by conformational changes on integrin [69] that result in the interaction with many signaling and structural proteins. Integrin-

fibronectin complexes cluster together on specialized nodes called focal contacts, where they aggregate with cytoskeletal adapter proteins called talin and vinculin on the cytoplasmic side of the cell membrane [67, 73]. These nascent adhesive structures mature into focal adhesions upon interaction with cytoskeletal proteins of which the most important is actin [73]. Ultimately, more than 50 different proteins can be found either stably or temporarily associated to focal adhesions, not to mention that many others can affect the structure of focal adhesions without being physically attached to them [74].

Focal adhesions are flat, elongated structures of several microns in length, often located on the periphery of cells. They mediate strong attachments to the substrate and anchor bundles of actin filaments [75]. Actin can be found in polymerized filaments or in monomeric form. Polymerization of actin supports plasma membrane protrusions [67]. This protrusion is the first step on a series of events taking part in cell adhesion, spread and migration processes [76]. Next, a cell attachment to a substratum takes place. This happens, for example, during the binding of fibronectin to integrins. Then focal adhesions are formed to link the substratum to the cytoskeleton. Finally traction is created in which the bulk of the trailing cytoplasm is drawn forward [77]. Ponti and colleagues determined that while lamellipodia formation is a random process caused by actin polymerization in a random trajectory, these temporary structures are disassembled quickly. Productive cell spreading takes place when lamillipodia formation is accompanied by adhesion to ECM ligands and formation of focal adhesions [76]. In addition, migration takes place when the process includes the disruption of older adhesion sites at the cell rear and cytoskeleton retraction [78]. The formation of actin fibers and recruitment of vinculin on focal adhesions are phenomena that were used to identify complete cell adhesion processes on the modified surfaces created in this study.

2.6 Cell Microenvironment Optimization in Tissue Engineering

The ultimate goal of tissue engineering is the restoration of organ and tissue function through the delivery of living components which become integrated into the patient [3]. The importance of this approach is clearly exemplified by the endothelialization of vascular grafts and its influence in the success of these devices [50]. Several approaches have been taken to promote cell adhesion, migration, proliferation and phenotypic differentiation on biomaterials [51, 63]. Such approaches can be mechanical, spatial, chemical or biological. For instance, Stegeman and Nerem report that, when exposed to different combinations of mechanical conditioning and exposure to growth factors, tubular collagen constructs seeded with smooth muscle cells changed their cell proliferation rate and alpha-actin expression levels. Cyclic mechanical strain also caused the seeded cells to align, and addition of different growth factors caused the construct to develop into looser or denser matrices [79]. There are numerous reports about the importance of scaffold architecture for cell support. Mandal and Kundu report that silk fibroin scaffolds of different porosities produce different rates of cell adhesion and proliferation. The spatial features of the scaffold influencing the cell population were not limited to pore size, but also included overall porosity and interconnectedness of the porous structures [80].

In a similar note, bioactive molecules have been added onto microenvironments and surfaces made from synthetic polymers. The simplest approach has been the passive release of these molecules from a source, such as porous polymeric matrices, that also serves as a substrate for cell growth [81]. A major inconvenience with this diffusible approach, however, is the instability of the concentration gradient. Chemical

immobilization can stabilize the distribution of these biomolecules [82, 83]. Shoichet and colleges, for example, reported that rat adrenal PC12 cells, which upon treatment with nerve growth factor (NGF) stop dividing and terminally differentiate [84], developed longer and stronger neurites when cultured on poly(2-hydroxyethylmethacrylate) [p(HEMA)] surfaces with chemically crosslinked NGF than on unmodified versions of this surface on the presence of soluble growth factor [85]. Prior to the development of their chemical immobilization method, a diffusible system was employed to study the neurite growth response to NGF concentration gradients. The unstable concentration in this type of diffusible system would pose great challenges for any *in vivo* application. The translation of these chemically crosslinked systems into therapeutical devices was the motivation behind the development of chemical crosslinking techniques [86].

Chemical immobilization of biofunctional peptides, such as those that promote cell adhesion, holds several advantages over diffusible passive adsorption from a biomaterial design standpoint [87]. First, covalent bonding is stronger and more stable than the interactions holding passively adsorbed peptides onto a surface, which can be overcome by shear forces, competitive adsorption with other proteins and proteolysis [88]. Second, the protein immobilization can be designed to preserve the accessibility of the peptide's binding site to cells, while passively adsorbed peptides might occlude the binding site [89, 90]. Finally, the choice of peptide and chemical linker can control directionality of the peptide, as well as the distance from the peptide to the surface [89].

With orthopedic and dental applications in mind, Petrie and colleges have successfully immobilized $FNIII_{7-10}$ and RGD-containing peptides onto titanium-coated surfaces by chemical means. This functionalization technique was applied on modified titanium implants *in vivo*, showing significantly improved functional oseointegration (as

measured by bone-implant contact area) with $FNIII_{7-10}$ presenting implants over those modified with RGD peptides and untreated ones [91].

Immobilization of cell-binding peptides has also been applied on crosslinked elastin-mimetic hydrogels. Kaufmann and Weberskirch, for instance, reported the immobilization of linear and cyclic RGD-containing moieties (oligopeptides conjugated to different spacers and functional groups) onto an elastic mimetic protein network. They used different crosslinkers for the elastin mimetic network and for the incorporation of RGD-containing moieties. They report that unmodified elastin mimetic hydrogels constitute inert surfaces to cell adhesion. The study also discusses the importance of the context on which RGD is presented, i.e. in linear or cyclic peptides and with or without the use of spacers [64]. Welsh and Tirrell have incorporated Arg-Asp-Gln-Val and RGD-containing peptides (both derived from fibronectin) directly into the primary sequence of their elastin mimetic protein by means of cloning. The crosslinkable elastin-mimetic and fibronectin-derived moieties have given these proteins the ability to form hydrogels of tunable mechanical properties and to support cell adhesion and migration [16, 92-94].

2.7 Crosslinking Agents

Crosslinkers are chemical reagents that create covalent or ionic bonds between polymer chains or, potentially, between segments of the same polymer chain. For the purpose of protein crosslinking, crosslinkers can be classified in three categories: heterobifunctional, homobifunctional and zero-length crosslinkers [95].

In general, crosslinkers react with functional groups on amino acid residues or with the carboxyl or amino terminal groups on proteins. In the case of heterobifunctional and homobifunctional crosslinkers, the reaction incorporates a covalent spacer between the two crosslinked groups. A homobifunctional crosslinker contains two identical reactive groups [96]. Examples of this category include 3,3´-Dithiobis (sulfosuccinimidylpropionate) (DTSSP) and pentanedial (glutaraldehyde) [97]. In contrast, a heterobifunctional crosslinker contains two different reactive groups [96]. These are more commonly used than homobifunctional crosslinkers, and some examples of this category include Dimethyl 3,3´-dithiobispropionimidate•2 HCl (DTBP) and Sulfosuccinimidyl 4-[N-maleimidomethyl]cyclohexane-1-carboxylate (sulfo-SMCC) [97].

When zero-length crosslinkers are used, a direct joining of two groups is induced without the introduction of any additional material, by, for example, the formation of an amide linkage, without the introduction of any extrinsic material. Some commonly used zero-length crosslinkers include carbodiimides like 1-ethyl-3-[3-dimethylaminopropyl] carbodiimide (EDC) that form amide linkages and others like cupric di(1,10-phenanthroline) and 2,2'-dipyridyldisulfide, that form disulfide bonds [96].

2.7.1 Genipin

For the purpose of this study, genipin was used to crosslink recombinant elastin meshworks and for the incorporation of rFN. Genipin is a naturally occurring crosslinking agent extracted from the fruits of the common gardenia (*Gardenia jasminoides*), a flowering tropical plant, and it is classified as an iridoid glucoside [98]. It is a crosslinker that reacts with primary amine groups. In protein crosslinking, it reacts mainly with the terminal primary amines in the side chains of lysine residues. Butler and colleges suggest that crosslinking takes place between primary amines and two reactive

sites in the genipin molecule. The first reaction is a nucleophilic attack of the genipin from a primary amine group that leads to the formation of a heterocyclic compound of genipin linked to the basic residue. The second reaction is a nucleophilic substitution of the ester group in genipin to form an amide link to the amino acid side chain and to release methanol. Genipin, however, also becomes polymerized in the crosslink formation through an oxidative reaction [99]. An inherent phenomenon in the crosslinking reaction is the oxygen radical-induced self-polymerization of genipin forming mixed short-range and long-range crosslink spacers, a reaction to which the blue pigmentation created by genipin is attributed [43, 98, 99].

Many other chemicals, including tannic acid, hexamethylene diisocyanate, glutaraldehyde, and dicumyl peroxide have been used in scientific research as crosslinking agents for recombinant elastin proteins [43]. However, one of the most compelling features of genipin is that its efficacy is comparable with that of glutaraldehyde, while the cytotoxicity of genipin-crosslinked gels and membranes is lower than glutaraldehyde-crosslinked or carbodiimide-crosslinked counterparts [98, 100].

Most importantly, genipin crosslinking modifies the mechanical profile of recombinant elastin proteins. It has been reported that after genipin crosslinking, recombinant elastin proteins form membranes whose approximated normalized modulus values (stress per strain per mass units) fall in range with values measured in aortic elastin [40, 43].

CHAPTER III

METHODOLOGY

3.1. Protein Production

3.1.1. Expression and Purification of Recombinant Elastin

The recombinant elastin protein used in this study, LysB10 was cloned into the pET24-a expression plasmid (Invitrogen, Eugene, Oregon) and transformed in the *E. coli* expression strain BL21(DE3). The design, cloning and transformation of the protein have been previously addressed by our group [35, 41]. Medium scale expression (16 L) were prepared in Circle Grow (MP Biomedicals, Solon, Ohio) medium at a pH of 7.5, supplemented with kanamycin (50 µg/mL) (Fisher Scientific, Fair Lawn, New Jersey) and incubated at 37°C with shaking.

Cells were harvested by centrifugation in sterile tubes at 1610 RCF for 20 minutes at 4°C, and the expression medium was discarded. The pellets were then resuspended in a total of 80 mL of cold sterile PBS (calcium and magnesium free) (HyClone, Logan, Utah). Cell fracture was performed with three freeze/thaw cycles at -80°C and 37°C. The cells were thoroughly lysed through six sonication cycles, each consisting of 20-second bursts, followed by 20-second resting periods in an ice bath. The lysate was centrifuged at 1660 RCF for 10 minutes at 4°C (Allegra 64 R, Beckman-Coulter, Fullerton, California) to recover any unbroken cells. The unbroken cells were resuspended in cold sterile PBS and sonicated again. The LysB10 protein was purified by inverse transition cycling [101].

The cell lysate was centrifuged at 20,000g for 40 minutes at 4°C (Sorvall RC-6 Plus model, Thermo Scientific, Ashville, North Carolina). The supernatant was transferred to cold sterile tubes and poly(ethyleneimine) (PEI) (Sigma-Aldrich, St. Louis, MO) was added to a final concentration of 0.5% and mixed gently with the lysate. After precipitation was observed, the lysate was centrifuged again at 20,000g for 40 minutes at 4°C for the removal of nucleic acids and other cell material. The supernatant was transferred to new sterile tubes and NaCl was added to a final concentration of 2M. The mix was, then, incubated at 25°C for 20 minutes to allow the elastin mimetic protein to coacervate and precipitate. Next, the mix was centrifuged at 8000g for 15 minutes (Beckman, J2-HS, Palo Alto, California) to separate the protein precipitate from the supernatant, which was then carefully decanted without disturbing the pellet. The protein was resuspended in cold, sterile PBS, shaken in a rotor incubator at 35 rpm for 5-10 minutes. The resuspended protein was centrifuged at 20,000g for 40 minutes at 4°C for 40 minutes again. The supernatant was transferred to 150 mL tubes and incubated at 25°C for 20 minutes. The mix was centrifuged at 8000g for 15 minutes, and the precipitate resuspended in cold PBS. This cycle of hot (25°C) and cold (4°C) spins was repeated until no contaminant pellet was observed after the cold spin. The number of cycles necessary was usually 8 or 9 and ended with a hot spin and resuspension.

Endotoxin removal required multiple sodium hydroxide (NaOH) treatments. Sterile NaOH (Sigma-Aldrich, Steinheim, Switzerland) was added to the resuspended protein to a final concentration of 0.4 N and mixed gently by hand. Then, sterile sodium chloride was added to a concentration of 2 M. These two last steps were performed under a cell culture hood and sterile techniques were employed. The protein was precipitated from solution at 25°C, and centrifuged at 8000g for 15 minutes at the same

temperature and resuspended in cold PBS (again, under sterile conditions). The endotoxyn removal treatment was repeated a total of three times.

Following the NaOH treatments, the protein solution was adjusted to pH 6-8. The solution was then sterile-desalted using PD-10 desalting columns (GE Healthcare Lifesciences, Piscataway, New Jersey) with molecular grade water (HyClone, Logan, Utah). The end product was syringe-filtered through a 0.2 µm filter (Millipore, Billerica, Massachusetts). Finally, solution was transferred into a 50 mL tube, frozen overnight at -80°C and lyophilized. The expression and purification processes produced white fibrous protein at a yield of approximately 35 mg per liter of expression culture.

3.1.2. Expression and Purification of Recombinant Fibronectin

The recombinant fibronectin protein used in this study, $FNIII_{7-10}$, was created by the Erickson group [54]. Using standard techniques, the DNA sequence coding for the protein was cloned into the XA3 expression vector plasmid (Pinpoint System, Promega, Madison, Wisconsin) by Petrie et al. [61] and kindly donated in plasmid form. The cloning resulted in the incorporation of a biotin-binding tag domain at the N- terminus of the protein. Type III domains 7 through 10 in fibronectin in addition with the biotin-binding domain add up to a total protein size of 52 kDa. The plasmid was transformed into JM109 *E. coli* expression strain (Promega, Madison, Wisconsin) by heat-shock treatment, as indicated in the manufacturer's specifications. After transformation, the cells were streaked onto LB agar plates (Beckton Dickinson, Sparks, Maryland) containing 100 mg/mL ampicillin (Sigma-Aldrich, St. Louis, Missouri). Single colonies were screened for successful transformants by standard gel electrophoresis and isolated. These colonies were then cultured overnight in LB broth with addition of 100 µg/mL ampicillin and 2 µM d-biotin (final concentrations) (Sigma-Aldrich, St. Louis,

Missouri), shaking at 225 rpm at 37°C. Overnight cultures were inoculated in a total of 2 liters of culture medium (same as above), and incubated until aliquots of the cultures had an optical absorbance of at least 0.8 at a wavelength of 600.00 nm. The cultures reached this point after approximately 5 hours. Protein expression was induced with Isopropyl beta-D-1-thiogalactopyranoside (IPTG) (Sigma-Aldrich, St. Louis, Missouri), added to a final concentration of 100 µM and incubation for 4 hours shaking at 225 rpm at 37°C.

Cells were harvested by centrifugation in sterile conical tubes at 1610 RCF for 20 minutes at 4°C, the expression medium was discarded. The cell pellets were stored at -80°C. The pellets were then resuspended in a total of 30 mL of PBS. Cell fracture was performed with three freeze/thaw cycles at -80°C and 37°C. For nucleic acid degradation, benzonase (Sigma-Aldrich, St. Louis, Missouri) and protease inhibitor cocktail (Sigma-Aldrich, St. Louis Missouri) were added to the cell resuspension. The cells were thoroughly lysed through ten sonication cycles, each consisting of 15 second bursts, followed by 30 second rests in an ice bath. Unbroken cells were removed by centrifugation at 3000g for 10 minutes and later at 13000 rpm for 20 minutes, in both instances, the temperature was kept at 4°C. The supernatant was syringe-filtered through a 0.2 µm filter. The volume of the lysate was reduced to approximately 15 mL using a 30,000 kDa pore-size centrifugal filter (Millipore, Billerica, Massachusetts). The protein solution was purified by affinity chromatography using an immobilized avidin agarose resin (Softlink Soft Release Avidin resin, Promega, Madison, Wisconsin) , which makes use of the avidin-binding tag attached to the protein, in a gravity column. For each purification, the column was washed with 8 volumes of PBS. After a 30-minute incubation, 0.5 resin volumes of cell lyste solution were added to the column.

Contaminants unbound to the resin were washed off with the addition of 35 volumes of PBS to the column. Afterwards, 4 resin volumes of 4 mM biotin were added

to elute all the biotin and biotinylated protein bound to the resin. The biotin excess was removed using 30 kDa centrifugal filters and PD-10 desalting columns. The protein was expressed and purified giving a yield of ~1 mg/mL. The protein purity was assessed at > 98% by Western blotting and Sodium dodecyl sulfate polyacrylamide gel electrophoresis (SDS-PAGE).

SDS-PAGE was performed on a 12% acrylamide gel (BioRad, Hercules, California) and total protein was visualized with Coomassie G250 (BioRad, Hercules, California). Western blot analysis was performed by transfer to an nitrocellulose membrane (BioRad, Hercules, California) and probed with mouse fibronectin monoclonal antibodies (HFN7.1) (Developmental Studies Hybridoma Bank, Iowa City, IA) followed by Amersham ECL™-HRP (horseradish peroxidase) linked goat-anti-mouse secondary antibodies (GE Bioscience, Piscataway, New Jersey) or streptavidin-alkaline phosphatase (Strep-AP) (Promega, Madison, Wisconsin). Bands were visualized by using an ECL Western blotting detection kit (GE Healthcare Lifesciences,) and Western Blue® stabilized substrate for alkaline phosphatase (Promega, Madison Wisconsin).

3.2. Cell Adhesion Experiments

3.2.1 Testing the Biological Activity of rFN

For all the surfaces used in cell adhesion experiments, non-tissue culture treated 96-well polystyrene plates were used (BD Falcon, Franklin Lakes, New Jersey). For the initial assessments of the biological activity of $FNIII_{7\text{-}10}$ (rFN), 100 µL of rFN or human plasma fibronectin (hpFN) (Invitrogen, Carlsbad, California) were added to each polystyrene wells and allowed to incubate overnight at 4°C. Unless otherwise specified, the coating concentration of rFN and hpFN was 50 µg/mL. After incubation, the wells were washed three times with PBS to remove non-adsorbed fibronectin. The wells

were, then, blocked with 1% bovine serum albumin (Fisher Scientific, Fair Lawn, New Jersey) for one hour at room temperature. Excess BSA was removed with three PBS washes. Each fibronectin-coated well constituted an experimental sample.

3.2.2. Preparation of LysB10 hydrogels

Untreated LysB10 gels (UTG surfaces) were prepared by hydrating dry fibrous LysB10 to a concentration of 60 mg/mL. The protein becomes soluble at cold temperature, so hydration required incubation at 4°C for 20-40 minutes with occasional vortexing. Bubbles were removed by centrifuging hydrated LysB10 at 13,000 rpm for 4 minutes at 4°C. For each experimental sample, 40 µL of hydrated LysB10 were carefully added to the bottom of a well in a 96-well polystyrene plate. This was performed in a cold room, at 4°C, to keep the protein liquid and prevent it from gelling. The viscous protein was equally spread on the bottom of the wells carefully without forming bubbles.

After laying the protein on the wells, the plates were incubated for one hour at 37°C to start protein gellation. At the end of the incubation, 200 µL of genipin at a 6 mg/mL concentration in PBS were added. The gels were allowed to crosslink overnight. Any unreacted genipin was thoroughly removed by washing the gels with fresh PBS three times. This triple PBS washing was repeated four times in the course of 12 hours for all the gel surfaces.

3.2.3 Passive Adsorption and Stable rFN Incorporation onto LysB10 Surfaces

For gel surfaces coated with passively adsorbed fibronectin (PAG surfaces), 100 µL of rFN solution were added on top of the gels, and the surfaces were incubated at room temperature overnight. Unless otherwise specified, the rFN coating concentration was 20 µg/mL.

Surfaces consisting of genipin-crosslinked rFN onto LysB10 gels (GPX surfaces) were prepared by incubating a solution of the desired concentration of rFN (20 µg/mL, unless otherwise specified) on top of LysB10 gels (before crosslinking) overnight. The following day, excess rFN was washed away with PBS, and 200 µL of genipin at a 6 mg/mL concentration in PBS were added on top of the gelled surfaces to crosslink rFN and LysB10 together overnight. Excess genipin was removed as previously described for untreated surfaces. For stability experiments, surfaces were washed with PBS daily for 7 days before cell adhesion experiments.

3.3. Cell Culture, Seeding and Quantification

Human umbilical vein cells (HUVEC) (Lonza, Walkersville, Maryland) cultures were started with approximately 250,000 cells in endothelial cell growth medium (EGM-2 BulletKit, Lonza, Walkersville, Maryland) in 75 cm2 flat culture flasks (BD Falcon, Franklin Lakes, New Jersey). The medium was replaced after 24 hours, the first time and, subsequently, after every 48 hours. After reaching 90-100% confluence, the cell cultures were washed three times with calcium-free, magnesium-free PBS, and the cells were detached using a PBS-based cell dissociation solution (Millipore, Billerica, Massachusetts). The cells were harvested by centrifugation at 2000 rpm for 7 minutes at 4°C (CR-312 model, Jouan, Winchester, Virginia). The cells were resuspended with HUVEC serum-free medium and any cell clumps broken by gentle shaking and occasional pipette suction until the cells were individually separate. Cells were seeded on protein-coated polystyrene wells and LysB10 gels at a number of 10,000 cells per well.

For proliferation experiments, the cells were seeded at a number of 5,000 per well. After two hours, the cell medium was switched, and fresh growth medium was

added on top of the cell-seeded surfaces. Cells were allowed to proliferate for a total of 48 hours. After 2 hours and 48 hours (for proliferation experiments) of incubation, the cell medium was removed, and unadhered cells were washed away with PBS. For cell fracturing, the plates were stored at -80°C overnight and thawed the following day. The cells were lysed and quantified using the CyQuant ® Cell Proliferation Assay Kit (Invitrogen; Eugene, OR), following the manufacturer's instructions. A CytoFluor® Series 4000 microplate reader (Applied Biosystems, Framingham, Massachusetts) was used to measure the fluorescence at an excitation of 485 nm and detection of 530 nm.

3.4 Elisa and rFN Immobilization Efficiency

An ELISA was used to determine the rFN immobilization efficiency. The Fibronectin EIA kit (Takara Bio; Otsu, Shiga, Japan) was used for these assays. The assay uses 96-well plates coated with FN30-8 capture antibodies and FN12-8 detection antibodies labeled with peroxidase (POD). These mouse antibodies, both directed to human fibronectin, were developed by Katayama et al. FN30-8 binds to a region encompassing amino acids in the $FNIII_8$ and $FNIII_9$ domains of fibronectin, between 153 and 229 amino acids away from the RGD site. FN12-8 antibodies bind to a region of fibronectin including amino acids in the $FNIII_{10}$ and $FNIII_9$ domains (not overlapping with FN30-8) [102]. This distribution assures that FN30-8 can be used to immobilize fibronectin without occluding the RGD or PHSRN sites, while these regions, so critical for cell-binding activity, can effectively be probed with FN12-8 antibodies. The antibodies were also reported by Katayama to not compete with each other in ELISA [102]. Furthermore, the epitopes of these two antibodies in fibronectin are reproduced in rFN, proving the compatibility of this commercially available assay with our recombinant version of fibronectin.

The FN30-8 –coated wells were used to immobilize rFN in the creation of a standard curve. GPX surfaces were prepared following the protocol explained before at different rFN concentrations. The assay was performed following the protocol specified by the supplier. For the standards, 100 µL of rFN at various concentrations were added to FN30-8 –coated wells, incubated for 1 hour at 37 °C and washed with a PBS solution containing 0.1 % Tween 20. For both standards and samples, FN12-8-POD conjugate solution was added to the wells. The plates were incubated for 1 hour at 37°C, and the wells washed. A buffered substrate solution containing hydrogen peroxide and tetramethylbenzidine (supplied by the manufacturer) was added and incubated for 15 minutes at room temperature. Finally, a 1N solution of H_2SO_4 was added to stop the reaction. The resulting absorbance at 450 nm was measured in a plate reader (Multiskan Spectrum model, Thermo Scientific, Ashville, North Carolina).

3.5. Immunostaining for Vinculin and Actin

Culture slides (BD Falcon, Franklin Lakes, New Jersey) were added hpFN and rFN for passive adsorption, blocked with BSA and seeded with HUVEC as specified before (see section 3.2.1 and 3.3). Similarly, hydrogel surfaces, untreated and rFN-modified, were prepared on culture slides and seeded with cells. Because of the interference of the blue coloration of genipin-crosslinked surfaces with the staining, the hydrogels were crosslinked with triglycidylamine, which produced transparent crosslinked surfaces. The crosslinker was synthesized by Venkat Krishnamurthy (Chaikof Lab) according to the protocol published by Connolly et al [103]. After a two-hour period of cell incubation, the surfaces were washed with PBS and fixed with 4% paraformaldehyde (PFA) for 10 minutes at room temperature. The surfaces were permeabilized with a PBS solution containing 0.5% Triton X-100 for 10 minutes at room

temperatures. The solution was removed, and the samples rinsed with a 100 mM glycine solution in PBS for 10 minutes at room temperature. The samples were then incubated with blocking buffer (PBS, 0.2% Triton X-100, 6% serum match to secondary goat antibody) with shaking for 1 hour at room temperature. For vinculin staining, mouse monoclonal antibody against human vinculin (Sigma-Aldrich, St. Louis, Missouri) was diluted in blocking buffer and incubated on the culture slides for one hour at room temperature with shaking. Samples were rinsed with blocking buffer and PBS. Secondary biotinylated goat anti-mouse IgG (Invitrogen, Eugene, Oregon) (2.5 µg/mL in blocking buffer) were added and incubated on the samples for 45 minutes at room temperature with shaking. After rinsing with PBS, the samples were added 2.5 µg/mL streptavidin-AlexaFluor 488 (Invitrogen) solution in PBS and allowed to incubate for 30 minutes. Cell nuclei were counterstained with Prolong gold mounting medium with DAPI (Invitrogen) and left to cure at room temperature protected from light for approximately 24 hours before sealing with nail polish.

For actin staining, AlexaFluor 568 phalloidin (Invitrogen) was diluted twenty-fold in PBS and added to the wells instead of primary vinculin antibodies. To reduce nonspecific staining, 1% BSA (final concentration) was added to this last solution. The samples were allowed to stain for 30 minutes. The samples were then rinsed with PBS. Counterstaining and curing steps were performed as in the vinculin staining protocol.

CHAPTER IV

RESULTS

4.1. Fibronectin and rFN Show Similar Biological Activity

Recombinant fibronectin, $FNIII_{7-10}$, was expressed and purified. The purity was assessed with a standard SDS-PAGE at >98% (Figure 4-1A). These PAGE results show a single noticeable band at the size expected for rFN (approximately 52 kDa). The presence of rFN in the purified sample was verified with western blotting and the addition of streptavidin alkaline phosphatase marker (Strep-AP). The marker binds to free biotin and to any biotin-binding molecule remaining after purification (Figure 4-1B). Only three possible biotin components were expected to be present in the cell lysate from the expression strain of *E.coli* used for this protein: free biotin (MW 244 Da), biotin carboxyl carrier protein (BCCP, a component of Acetyl-CoA) (22.5 kDa) [104] and biotinylated rFN (52 kDa).

Finally, identity of the purified recombinant expression product was confirmed by western blotting and immunostaining (Figure 4-1C). HFN 7.1 mouse fibronectin monoclonal antibodies were used in this experiment as primary antibodies. This antibody maps to the cell-binding region of fibronectin between the ninth and tenth type III repeat, and it is capable of blocking cell adhesion to fibronectin [105]. Keselowski, Petrie and Garcia describe the correlation between HFN7.1 binding and the availability integrin-binding sites in fibronectin and, therefore, fibronectin's biological activity [61, 106]. The

results for all of the three tests, SDS-PAGE, Strep-AP and immunostaining showed a single dominant band at the expected size.

The biological activity of rFN and its similarity with hpFN were assessed directly through cell adhesion assays. Polystyrene surfaces were coated rFN and hpFN by passive adsorption. HUVECs were seeded and the number of cells adhering to the protein-coated surfaces was measured. Adherent cells were fixed and stained for vinculin and actin. Morphological characteristics of cell adhesion were observed in both rFN- and hpFN-coated surfaces by immunostaining (Figure 4-2).

The adhesion assay results (Figure 4-3, Mean ± S.D.; n=4), showed that rFN- and hpFN-coated surfaces have the same degree of cell-binding activity. The adsorption of both proteins improves cell attachment onto an otherwise inert surface.

The activity of rFN was further compared to that of hpFN by observing how protein coating concentration influences the biological activity of the surfaces in both cases. Different concentrations of rFN were passively adsorbed onto polystyrene surfaces, and the number of cells adhering to these surfaces was measured (Figure 4-4, Mean ± S.D.; n=4). The number of adhered cells reached a plateau after a coating concentration of 5 µg/mL, which is in agreement with results published for hpFN concentration gradients by Lightner and Erickson [107] and with results other results published for rFN concentration gradients by Cutler et al [108].

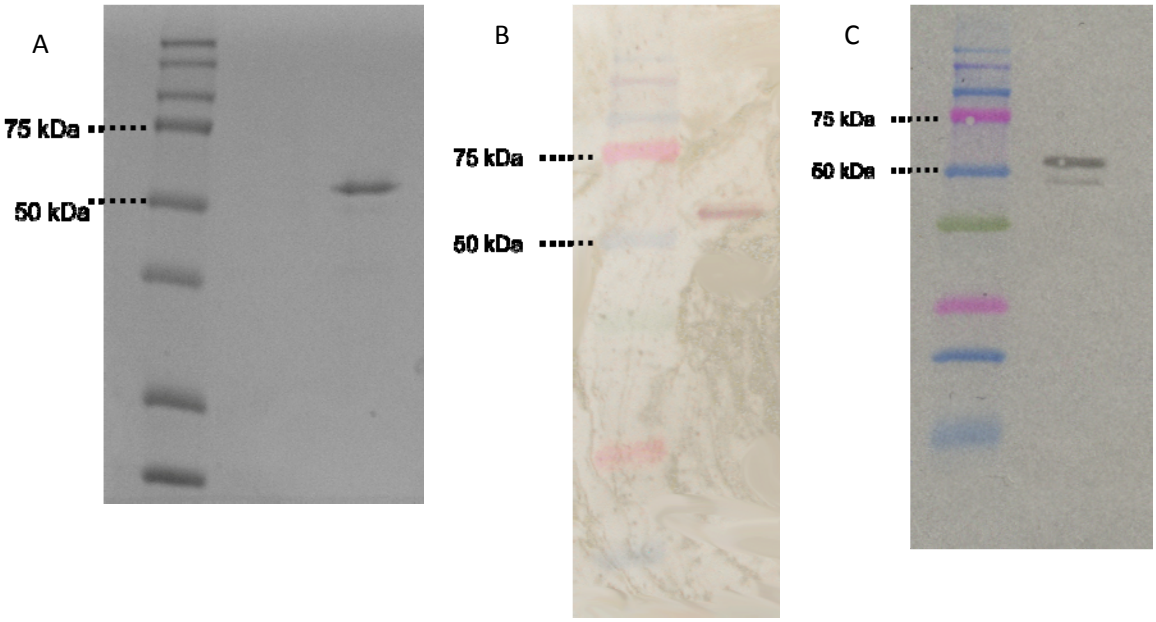

Figure 4-1. Purification of rFN. (A) SDS-PAGE. (B) Western blot with streptavidin alkaline phosphatase marker. (C) Western blot immunostained with HFN7.1 (fibronectin binding) primary antibody and HRP-conjugated goat anti-mouse) secondary antibody marker.

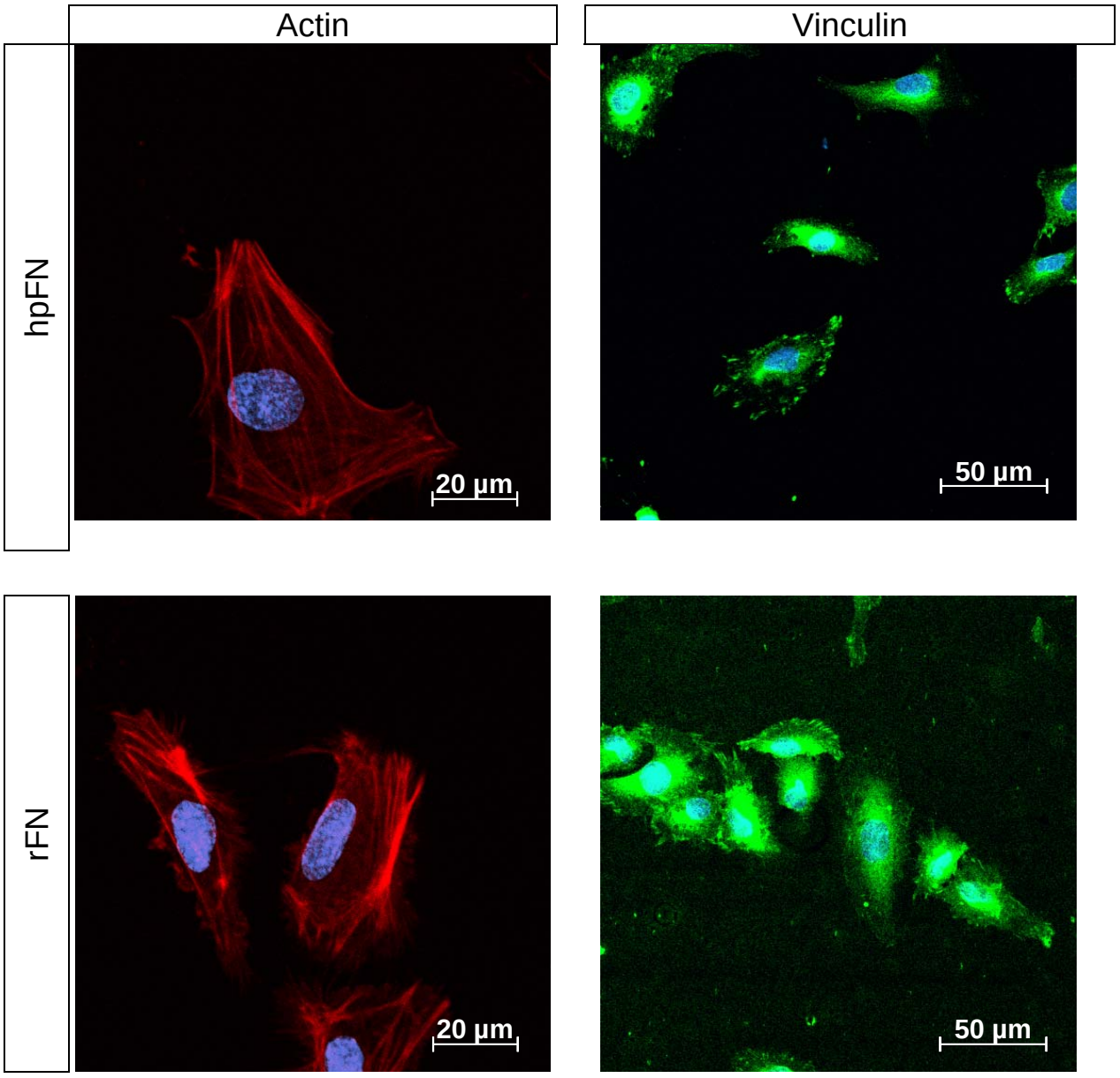

Figure 4-2. Immunostaining for cell adhesion activity to rFN and hpFN. Polystyrene surfaces were coated with hpFN and rFN and seeded with HUVECs. Adhered cells were fixed, permeabilized with 0.5% Triton X-100, stained for vinculin and for actin to visualize actin filaments and focal adhesions and counterstained with DAPI.

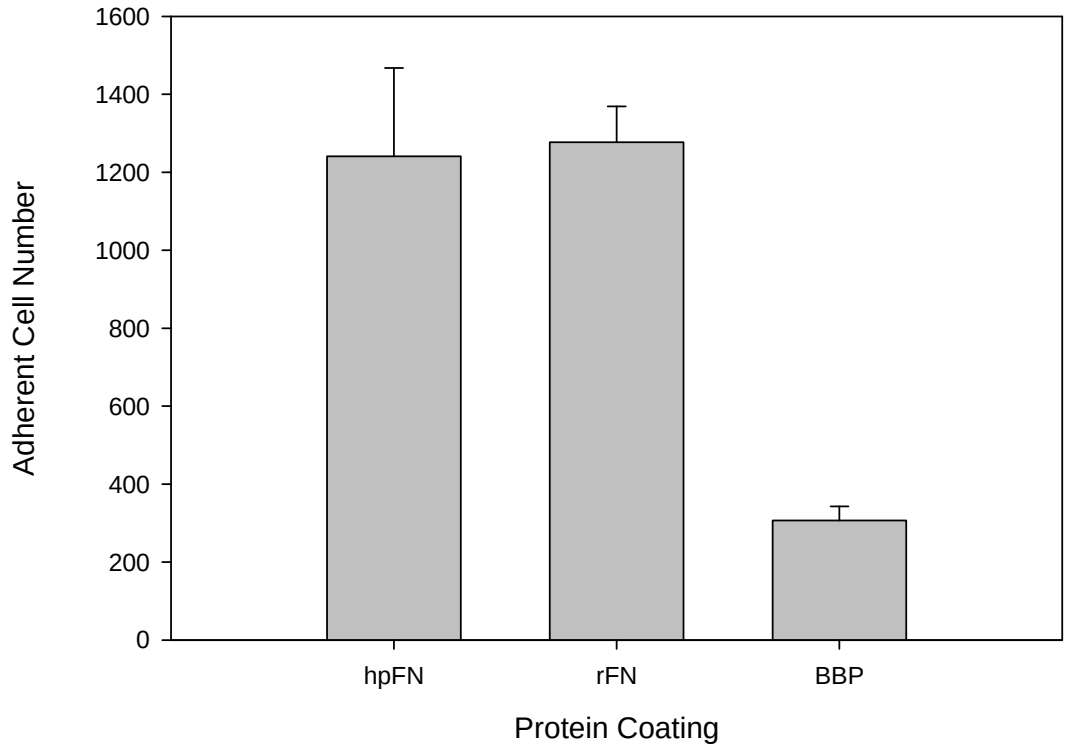

Figure 4-3. Cell-adhesive activities of rFN and hpFN compared. The two fibronectin variant proteins were passively adsorbed onto polystyrene surfaces at a concentration of 50 µg/mL. Inert BSA-blocked polystyrene (BBP) surfaces were used as negative controls (n=4).

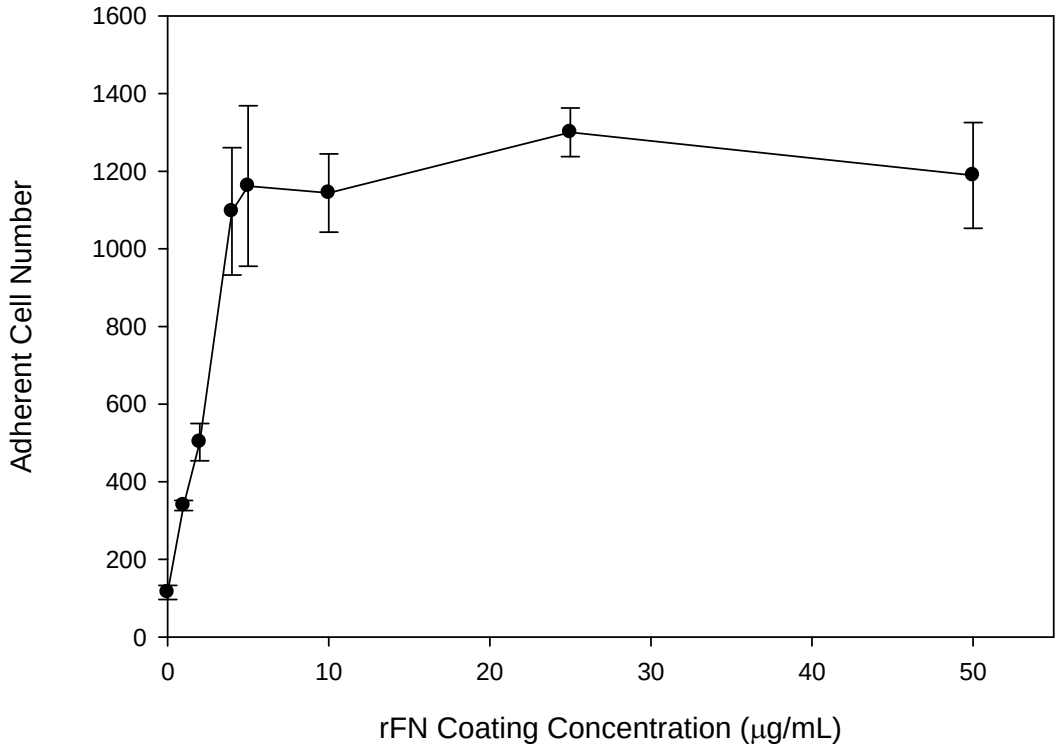

Figure 4-4. Cell-adhesive activity of rFN at different coating concentrations. Recombinant fibronectin at different concentrations was passively adsorbed onto polystyrene wells. Polystyrene surfaces were then blocked with BSA. Cell adhesion to these rFN-coated surfaces was measured (n=4).

4.2. LysB10 Hydrogels Cannot Support Cell Adhesion

In order to demonstrate that recombinant elastin hydrogels do not support cell adhesion on its own, LysB10 in soluble phase was added to polystyrene wells. Gels were formed by allowing the soluble protein to coacervate at higher temperatures, and then chemically crosslinking them with genipin. Unreacted genipin was thoroughly washed to ensure cell membrane proteins would not be crosslinked into the hydrogels and cell adhesion results would not be skewed. No rFN was added to untreated gel (UTG) surfaces. Crosslinked LysB10 gels showed low levels of cell adhesion in comparison with rFN-coated polystyrene, yet higher than untreated polystyrene (Figure 4-5, Mean ± S.D.; n=4-7).

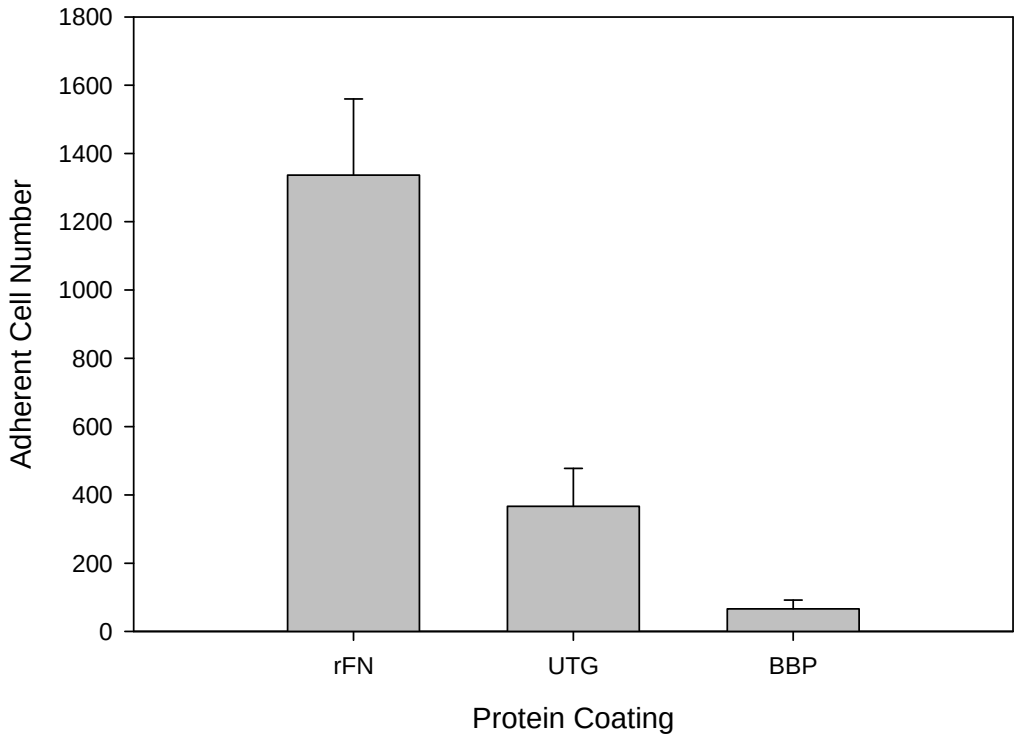

Figure 4-5. Cell adhesion to LysB10 hydrogels. HUVECs were seeded on genipin-crosslinked LysB10 gels with passively adsorbed rFN (50 µg/mL) onto polystyrene (rFN column), BSA-blocked polystyrene (BBP) and on genipin-crosslinked LysB10 gels without rFN (UTG) (n=4-7).

4.3. LysB10 Hydrogels Support Cell Adhesion in the Presence of rFN

As proof of concept that rFN can improve the cell-adhesive activities of LysB10 surfaces, rFN was passively adsorbed onto the surfaces. To demonstrate that improvements in cell adhesion were due to the presence of rFN on the gels, the fibronectin variant was incubated at different concentrations. Once again, an increase on rFN coating concentrations generated an increase in the number of cells adhered to otherwise more sterile surfaces (Figure 4-6, Mean ± S.D.; n=3-4). HUVEC adhesion to LysB10 was low (though greater than to untreated BSA-blocked polystyrene), but greatly improved in the presence of rFN.

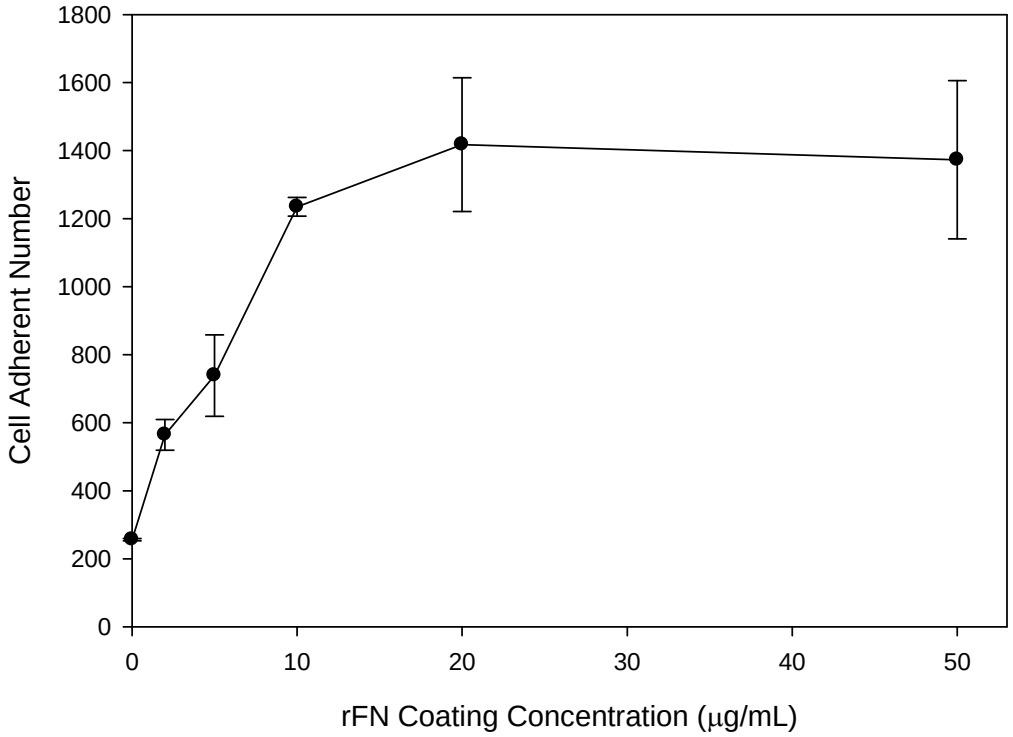

Figure 4-6. Improvement of cell adhesion on LysB10 hydrogels in the presence of rFN. Different concentrations of rFN were used to coat LysB10 hydrogels. Adherent cell numbers were measured (n=3-4).

4.4 LysB10 Can Be Stably Modified with the Incorporation of rFN

Once it was observed that rFN could increase the adhesion of endothelial cells to LysB10, stable methods for modifying hydrogels were explored. Prior to genipin crosslinking, rFN solutions were incubated on top of coacervated LysB10 gels. Then genipin was added to crosslink rFN and LysB10 networks together. The rFN immobilization efficiency was determined by means of an ELISA. GPX surfaces were probed with POD conjugated fibronectin antibodies, and the absorbance was measured. The assay showed a hyperbolic relation between the rFN concentration coated on coacervated LysB10 prior to genipin addition and rFN effectively immobilized (Figure 4-7, Mean ± S.D.; n=3). Cell morphology characteristics associated with adhesion were identified by fixing adherent cells and staining them for actin. Cells adhered to modified surfaces presented actin filaments traversing stretched cytoplasms. In contrast, cells adhered to unmodified surfaces presented a round shape with actin dispersed throughout the cytoplasm (Figure 4-8).

The cell adhesion levels of the rFN-LysB10 genipin crosslinked surfaces (GPX) were compared with passively adsorbed rFN onto LysB10 and rFN-free LysB10 hydrogels. The chemically modified surfaces showed the same cell-binding effectiveness as coated hydrogel surfaces. The incorporation of rFN by means of chemical crosslinking or absorption greatly increased cell adhesion on hydrogels (Figure 4-9, Mean ± S.D.; n=4).

The effects of rFN concentration on the cell-adhesive ability of GPX surfaces were studied. A dilution series of rFN was prepared and different concentrations were used during the incubation of coacervated LysB10 gels, prior to genipin crosslinking.

The relation between rFN concentration and cell adhesion shows a hyperbolic curve similar to the one observed for rFN coated hydrogels (Figure 4-10, Mean ± S.D.; n=3).

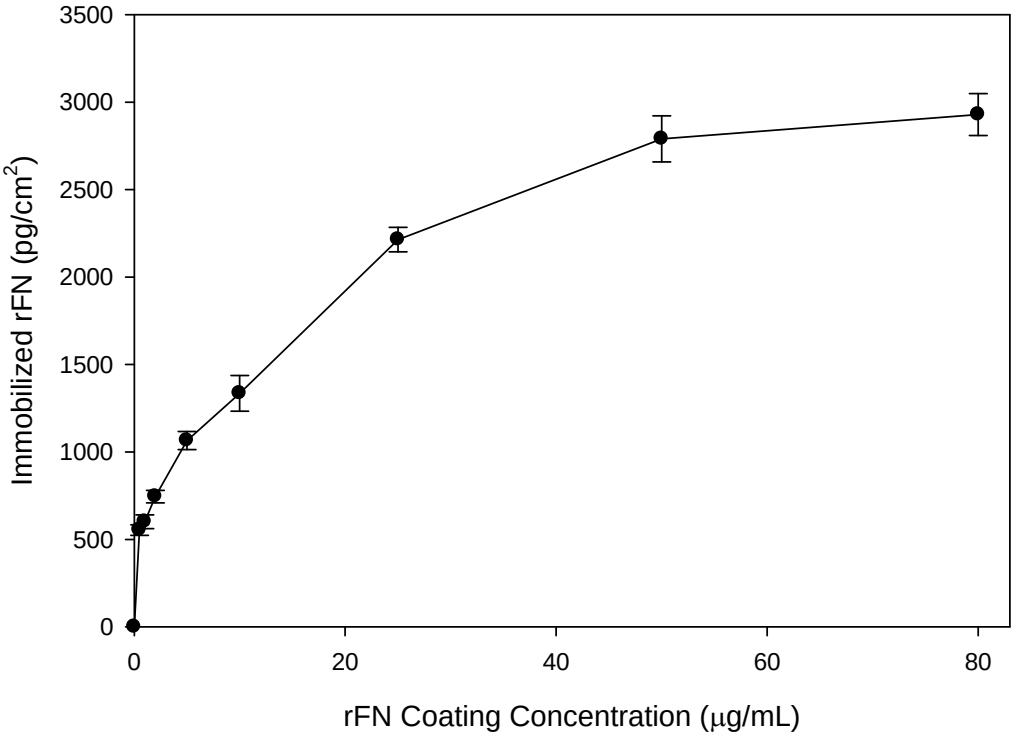

Figure 4-7. Crosslinking efficiency of rFN onto LysB10 hydrogels. Amounts of rFN immobilized in GPX surfaces were measured using a sandwich ELISA. FN30-8 capture antibodies and HP12-8-POD conjugate detection antibodies were used for standard immobilization and for probing, respectively (n=3).

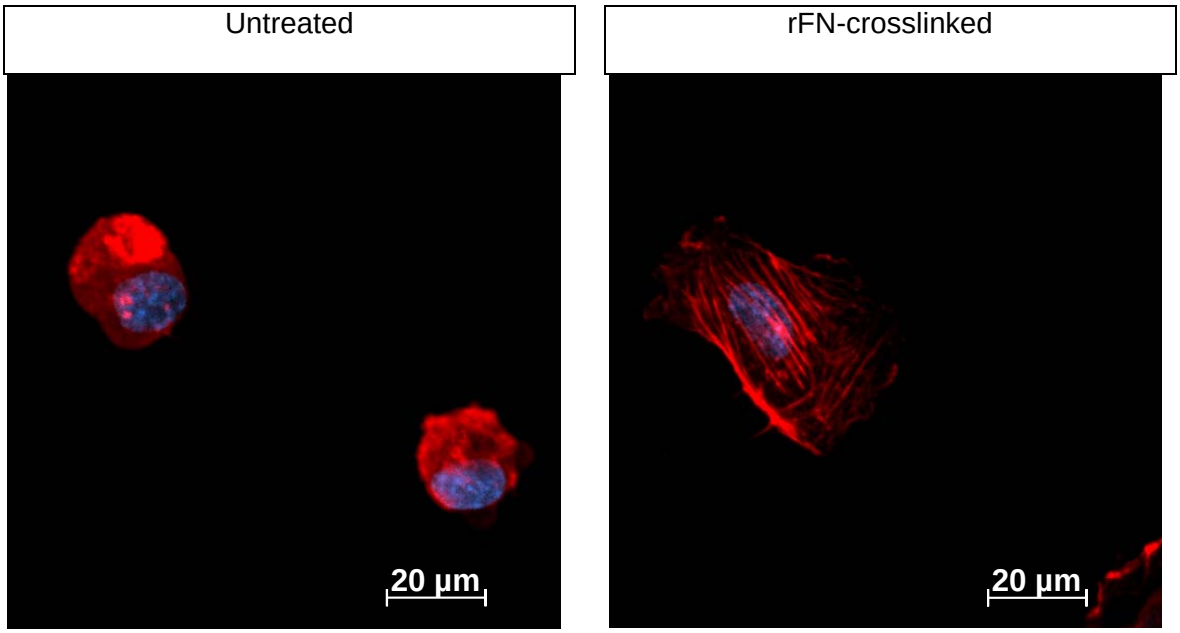

Figure 4-8. Immunostaining for cell adhesion activity to untreated and modified hydrogels. Untreated and rFN-crosslinked gel surfaces were prepared as explained and seeded with HUVECs. Adhered cells were fixed, permeabilized with 0.5% Triton X-100, stained for actin and counterstained with DAPI.

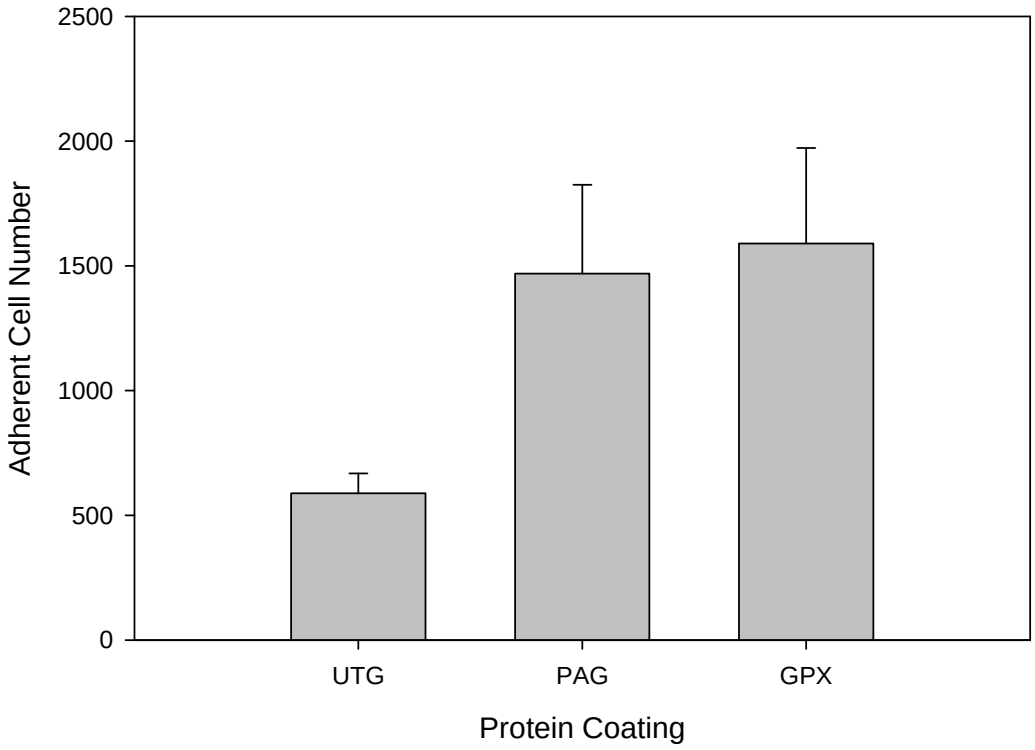

Figure 4-9. Cell adhesion to modified LysB10 hydrogels. HUVECs were seeded on three types of hydrogel surfaces: chemically modified rFN-LysB10 hydrogels (GPX), rFN coated (PAG) and untreated hydrogels (UTG). (n=4).

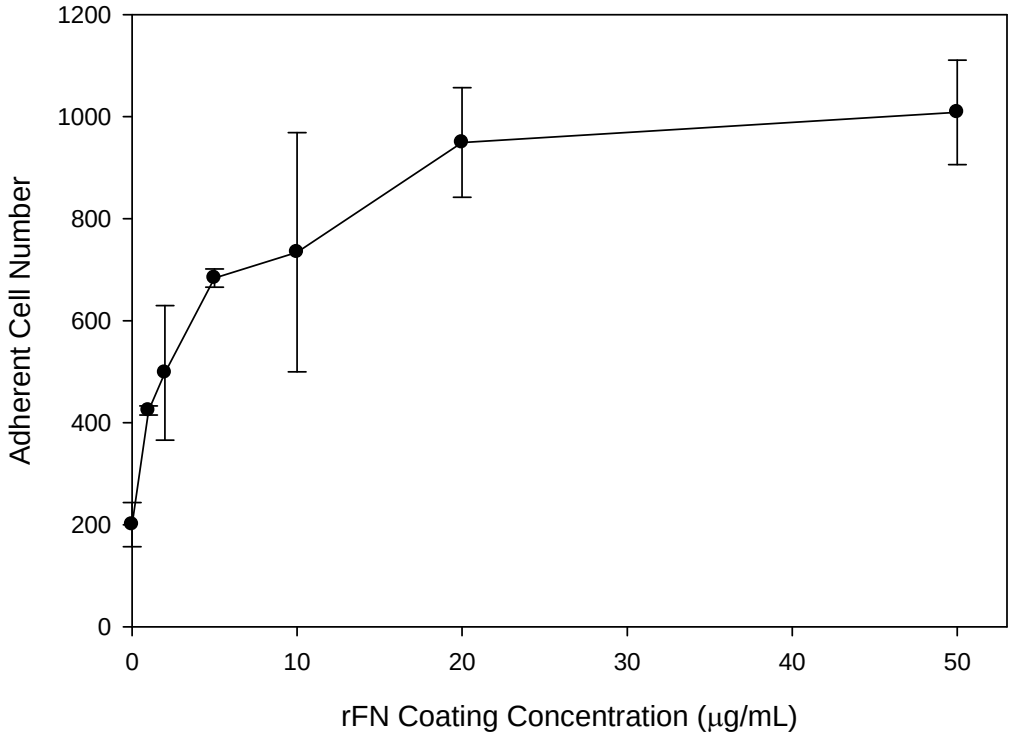

Figure 4-10. Cell adhesion to modified LysB10 hydrogels at different rFN concentration. Different concentrations of rFN were incubated on top of LysB10 prior to chemical crosslinking. Higher incubation concentrations resulted in greater adhesive cell numbers (n=3).

The potential of modified hydrogels for endothelialization was further assessed by observing the surface's suitability to sustain cell proliferation. GPX and PAG surfaces were prepared as previously specified. Cells were seeded and incubated for a period of 2 and 48 hours. At t=2 hours, non-adhered cells were washed away and the adhesion (basal) medium was exchanged for HUVEC growth medium. The adherent cell number was measured at t= 48 hours (Figure 4-11, Mean ± S.D.; n=3). The proliferation rate was calculated by normalizing the cell number at 48 hours over the number of cells adhered to the surfaces at the beginning of the incubation period (t=2 hours). Both surfaces showed a comparable proliferation rate. The number of cells on both surfaces had more than doubled in the course of 48 hours of incubation.

Finally, the superior stability of chemically modified hydrogels over coated hydrogels was verified by means of a prolonged surface incubation. UTG, PAG and GPX surfaces were prepared and kept hydrated with PBS during seven days of incubation. The PBS was replaced daily during that period. At the end of the incubation, HUVECs were seeded as normal and adherent cell levels were measured. The chemically modified surfaces retained their whole cell adhesive ability. On the other hand, the adhesion levels on coated hydrogel surfaces dropped closed to the levels in unmodified gel surfaces, losing their ability to support cell adhesion (Figure 4-12, Mean ± S.D.; n=4).

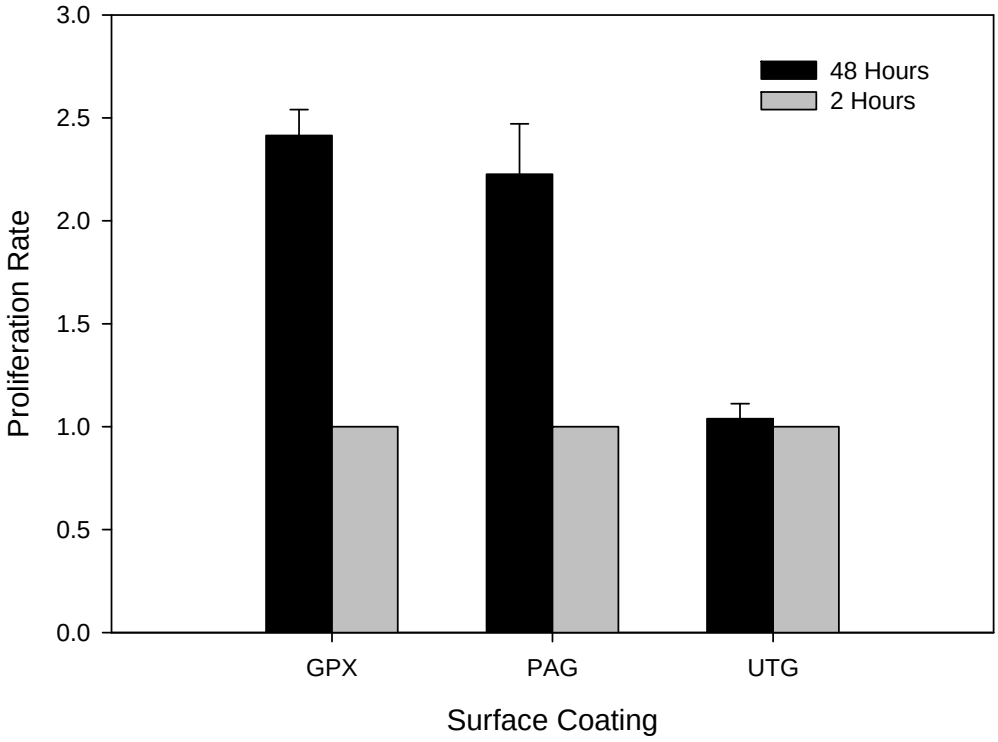

Figure 4-11. Endothelial cell proliferation on modified, coated and untreated hydrogels. HUVECs were seeded on chemically modified (GPX), rFN coated (PAG) and untreated (UTG) hydrogels. Cells were allowed to adhere to the surfaces for the first two hours after seeding. Non-adherent cells were washed away and growth medium was added on the hydrogels to allow for cell proliferation. The proliferation rate at 48 hours after seeding was calculated based on adherent cell levels before proliferation (n=3).

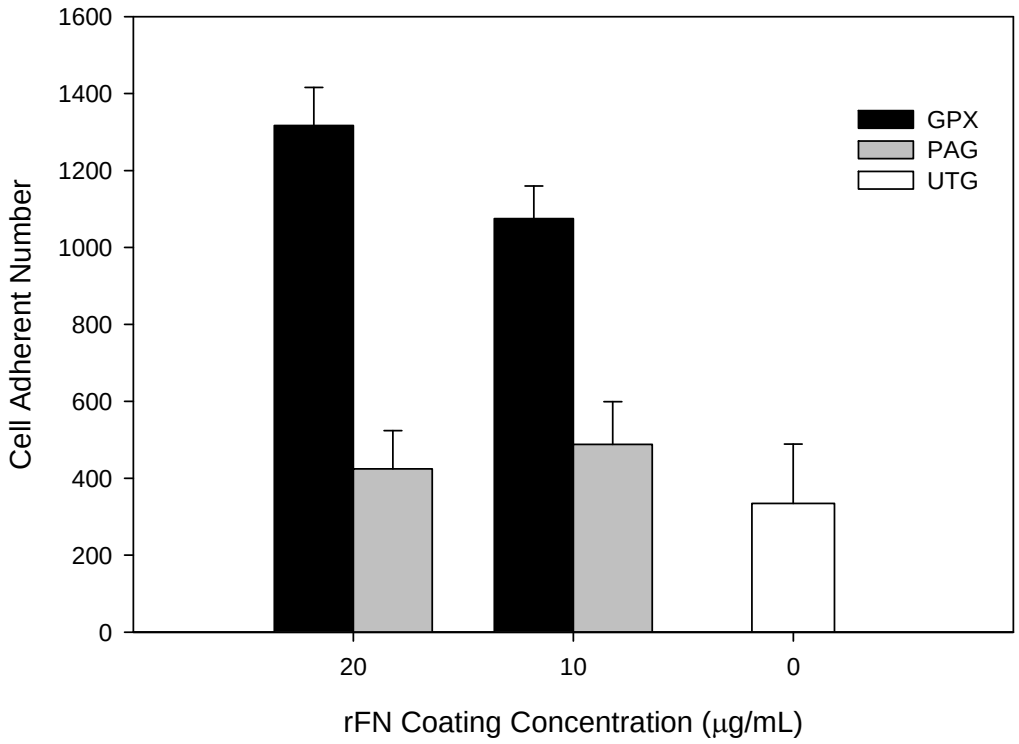

Figure 4-12. Stability of the chemical modification of hydrogels. Three types of hydrogel surfaces were prepared: chemically modified rFN-LysB10 hydrogels (GPX), rFN coated (PAG) and untreated hydrogels (UTG). Prior to cell seeding, the gels were kept hydrated and in incubation for seven days. Hydration medium was changed daily during that time. Cell adhesion levels were measured at the end of the incubation period (n=4).

CHAPTER V

DISCUSSION

This work describes the chemical incorporation of a recombinant fibronectin protein into an elastic mimetic hydrogel. Elastin was chosen as a substrate protein because of the role it plays in the mechanical profile of native vasculature [23, 33]. Several forms of recombinant elastin have been developed based on well studied conserved amino acid repeat sequences in native elastin [36, 41]. One of the main appeals for the use of recombinant versions of elastin is the possibility of tuning macroscopic properties of the protein by changing its primary sequence [38] and well optimized purification protocols [101]. LysB10 is an amphiphilic version of this protein previously created and characterized by our group. LysB10 was designed to include the crosslinking capabilities of native elastin and a coacervation point at physiologically relevant conditions [41].

$FNIII_{7-10}$ was chosen for this study due to its well studied ability to reproduce the cell adhesive properties of human plasma fibronectin [108] by means of the inclusion of RGD, an important cell-binding peptide [54] and PHSRN a peptide sequence that plays a synergistic role to RGD in cell adhesion [60, 61]. While other groups have worked on the incorporation of small RGD-containing peptides, these show a significantly lower cell adhesive activity compared to the complete protein [108]. Grant and colleagues have shown that not only the presence of RGD and PHSRN is necessary to obtain complete cell adhesive activity, but that alterations in the positioning of these sites with respect to each other can reduce cell attachment, spreading and downstream signaling events in the cell [109]. This recombinant version of fibronectin was chosen over native

fibronectin due to the possibility of introducing modifications by means of genetic engineering. One of these modifications was the addition of a biotin-binding domain by Petrie and colleges [61]. The addition of this domain allowed for a simplified purification of the protein with commercially available purification kits. The engineered biotin-binding ability can also be used for specific, sensitive and facile detection, quantification, as well as new forms of protein immobilization taking advantage of the well known biotin-streptavidin interactions [110]. This last concept was explored by McDevitt and colleagues. RGD-containing recombinant fibronectin was cloned into recombinant streptavidin. The resulting fibronectin-streptavidin protein was immobilized onto polystyrene surfaces blocked with biotinylated BSA, which effectively increased cell adhesion onto the surfaces in a manner dependent on the concentration of the recombinant protein [111].

Immunostaining for vinculin and actin indicate that cells adhered to rFN and to hpFN present the same morphology. Furthermore, these morphological features in the cells are characteristic of focal adhesion formation and cell spreading. Focal complexes are formed after the binding of fibronectin and integrin on the cell membrane. Fibronectin-integrin complexes are recruited and a signaling process takes place, resulting on the recruitment of vinculin and other proteins on the intracellular side of the membrane.

The immunostaining results for surfaces coated with hpFN and rFN display a greater concentration of vinculin on discrete point locations, mostly on the periphery of the cell [75]. The distribution of vinculin in these images suggests the protein is being recruited for the formation of focal adhesions. Actin staining shows a fibrous mesh formed across a stretched cytoplasm on hpFN and rFN surfaces. This morphology is expected from the polymerization of actin and the formation of stress fibers as the cell

binds to fibronectin on a rigid substratum and spreads. The same actin morphology was observed when cells adhered to modified LysB10 surfaces were stained with phallopoid, indicating cell adhesion events. As expected, cells adhered to hydrogels that did not present rFN remained rounded in shape and did not form a fibrous mesh of actin fibers.

Bix et al. performed reported that endorepellin (the C-terminal domain of the heparan sulfate proteoglycan perlacan) and one of its modules are capable of disrupting focal adhesion formation and actin stress fibers. Their immunostaining results constitute a good source of comparison with those obtained in this study. Untreated controls and cells after a 3-hour recovery show vinculin and actin morphologies similar to the results obtained in this study and described above. In contrast, cells exposed to endorepellin and fixed without allowing for recovery show vinculin dispersed throughout the cytoplasm rather than concentrated on focal adhesions. Similarly, actin is not present in the form of filaments, but it is, instead, spread throughout the cytoplasm. Nevertheless, actin seems to concentrate on intercellular junctions rather than on focal adhesions [112].

In this study, genipin was the crosslinking agent of choice for the chemical crosslinking of LysB10 hydrogels and the incorporation of rFN. Glutaraldehyde is the most commonly crosslinking agent for proteins [100], including elastin mimetic proteins [41, 92]. Genipin has been reported to have efficacy levels similar to glutaraldehyde with a much lower cytotoxicity [43]. The mechanical enhancements glutaraldehyde produces on LysB10 have been extensively documented by Sallach and colleges. Their findings include a doubling of the material's Young modulus, increases in the ultimate tensile strength and decrease of its strain at failure [41]. Genipin crosslinking of EP20-24, another elastin-mimetic protein developed by the Keeley group [40], has produced membranes whose normalized modulus values fall in range with values measured in

aortic elastin [43]. In comparison with LysB10, however, the sequence EP20-24 is shorter and richer in crosslinkable amino acid residues. It is necessary to perform mechanical tests on genipin-crosslinked LysB10 hydrogels. While a stiffening of the material is clearly expected, the tests will determine if the mechanical profile of the crosslinked hydrogels is comparable to natural elastin vasculature.

One of the hypotheses of this study was that rFN has comparable biological activity to that of hpFN. The results obtained in this study show that both proteins, when passively adsorbed to polystyrene surfaces, provide increased support for cell adhesion at comparable levels. These results are in agreement with those shown by Erickson [107] and by Garcia [108] in direct comparison. Furthermore, in this work the same hyperbolic relation is shown between the coating concentration of rFN and the number of adherent cells as published by Erickson [107]. In both studies, cell adhesion plateaus at a concentration of approximately 5 μg/mL.

It was observed in this research that LysB10 hydrogels do not support cell adhesion. While peptide sequences with chemotactant effects over fibroblasts and monocytes have been identified in natural elastin [113], recombinant elastin substrates have generally not been reported as capable of supporting cell adhesion [64, 114]. The only exceptions to these reports are cases where cell-binding peptides derived from other ECM proteins have been incorporated into the primary sequence of the elastin-mimetic protein [93, 94] or when a spatially (rather than biochemically) suitable environment has been created for cells by means of electrospinning a fibrillar network [29]. Urry and coworkers, stated that preliminary data on certain elastin mimetic proteins (specifically, VGVGP repeats) indicated they were refractive to cell adhesion, opting, instead on the incorporation of RGD sequences into the protein for cell-binding effects [115].

Hydrogels coated with rFN and covalently modified with rFN initially had comparable levels of cell adhesion. A stability test was performed to determine whether these forms of rFN presentation lead to stable surface functionalization. After a long incubation period, only surfaces chemically modified with rFN retained biological activity. To our knowledge, protein adsorption onto elastin mimetic substrates has not been studied. Due to the high hydrophobicity of elastin [36, 44] and its recombinant analogs, however, high levels of protein adsorption are possible on the basis of lower interfacial energies towards the biological surroundings than to an aqueous medium [116]. As one of her controls Kaufmann reports negligible levels of cell adhesion onto an elastic mimetic surface incubated in the presence (but not chemically coupled) to an RGD-containing peptide [64]. This however, is an oligopeptide of 6 residues, compared to the 52 kDa size of rFN, which could account for the negligible levels of cell adhesion to unmodified substrates.

The experiments on the stability of chemical modification showed that surfaces coated with rFN do not retain biological activity after long incubation prior to cell seeding. This indicates that only chemical modification provides a stable and reliable method for increasing endothelialization of LysB10 hydrogels. Chemical immobilization holds several advantages over diffusible passive adsorption from a biomaterial design standpoint. Even though cell-binding peptides have been used to coat inert surfaces and produce adhesive substrates in the short term [65], passive adsorption is not suitable for materials exposed to protein solutions, such as cell culture medium for long times, since desorption and proteolysis of the non-covalently bound protein can occur in addition to competitive adsorption with serum proteins [87, 117]. Covalent bonding is stronger and more stable than the interactions holding passively adsorbed peptides onto

a surface, which can be overcome by shear forces, competitive adsorption with other proteins and proteolysis [88].

During the chemical modification of hydrogels, genipin crosslinks rFN proteins coating coacervated gels. Excess protein (not adsorbed onto the gels) was removed by washing prior to the addition of genipin. The effects of protein concentration on cell adhesion with passively adsorbed rFN and chemically modified surfaces show the same hyperbolic relation. Both curves plateau at rFN concentrations of approximately 20 µg/mL. This approach could, ultimately, achieve the stable blocking of the hydrogel surfaces with cell-binding proteins.

The rFN crosslinking efficiency was assessed by ELISA. The assay further supports the observation of concentration-dependent functionalization of LysB10 as seen on coated and modified hydrogels. Protein concentration and effective immobilization displays a hyperbolic relation similar to that seen between concentration and cell adhesion. The ELISA results in this study are in agreement with results published by Garcia et al., who also report this hyperbolic relation [61]. Furthermore, the maximum amount of rFN immobilization per surface area in this study is in the same order of magnitude as that reported by Petrie (~3000 ng/cm^2 and ~6500 ng/cm^2, respectively), though a different crosslinking method was used. These results are comparable to reports by Zhang et al, who immobilized hpFN onto aminized PET using glutaraldehyde as the crosslinking agent. They obtained the equivalent of approximately 45 femtomoles of immobilized hpFN at a concentration of 30 µg/mL [118]. Roughly the same result was obtained in the ELISA performed for this study when differences in molecular weight of rFN and hpFN (52000 and 440000, respectively) are taken into account.

Another approach taken for the immobilization of recombinant fibronectin proteins onto substrates was that taken by McDevitt et al. Fibronectin-streptavidin recombinant protein was successfully immobilized onto polystyrene sufaces blocked with biotinylated BSA. Rat aortic endothelial cell adhesion showed not the hyperbolic relation to protein concentration observed in this study with HUVECs, but instead described a sigmoidal curve. Cell adhesion plateaus at a protein concentration similar to modified surfaces in this study (~ 14 and 20 µg/mL respectively) [111]. McDevitt reports cell adhesion in absorbance levels rather than cell number, so more specific comparisons about cell adhesion levels cannot be made. It is important to notice, however, that the fibronectin-derived RGD sequence incorporated into this protein is only 8 amino acids long (compared with 369 in rFN) and does not contain the PHSRN synergy site.

Tirrell and coworkers have taken a different approach to the incorporation of fibronectin segments onto elastin-mimetic proteins [16, 92-94]. Instead of chemical immobilization, they have opted for engineering fibronectin peptide segments directly into the primary sequence of their recombinant elastin segment. One of the advantages of this approach is that fibronectin grafting efficiency is directly controlled by the frequency cell-binding sequences repeat in the protein design in comparison with a more difficult control of crosslinking reactions. On the other hand, Liu and Tirrell, inserted only RGD sequences in their protein [93], while the PHSRN synergistic site, and in the correct positioning, is required to elicit the full effect of cell adhesion in both efficacy and signaling cascade activity levels, [108, 109]. In addition, access to the cell-binding site is limited. The RGD peptide is presented only at surface level and with very limited mobility. With the crosslinking of rFN onto hydrogels, the length of the protein, approximately 140 angstroms [59] if grafted from near the n-terminus, serves as spacer and increases mobility, thereby increasing the access to the cell binding sites.

In this study, elastin mimetic surfaces were successfully functionalized with recombinant fibronectin. The unmodified surfaces initially showed an inability to support cell adhesion. Chemical crosslinking of rFN onto these substrates conferred elastin mimetic hydrogel sufaces with the ability to support cell adhesion and proliferation. The biological activity of rFN was studied and compared with natural human plasma fibronectin prior to any chemical incorporation. It was observed that rFN promotes similar levels of cell adhesion as natural fibronectin. Furthermore, the relation between cell adhesion and protein concentration was determined to be similar for recombinant and for natural fibronectin. HUVECs showed the same morphology when adhered to inert surfaces coated with either type of fibronectin. Later, rFN was implemented on LysB10 hydrogels, where surface coating promoted cell adhesion and proliferation. Finally, rFN was chemically immobilized onto the hydrogels. The same biological effects were observed in modified and coated surfaces. Adhered cells also showed the morphology characteristic of cell adhesion. The immobilization efficiency of the technique used in this study was found to be comparable with others reported in the literature. Chemical immobilization, unlike passive adsorption, proved to be a stable form of elastin mimetic hydrogel functionalization for promoting endothelialization.

REFERENCES

1. Lloyd-Jones, D., et al., *Heart disease and stroke statistics--2009 update: a report from the American Heart Association Statistics Committee and Stroke Statistics Subcommittee.* Circulation, 2009. **119**(3): p. 480-6.
2. DeFrances, C.J., et al., *2006 National Hospital Discharge Survey.* Natl Health Stat Report, 2008(5): p. 1-20.
3. Vacanti, J.P. and R. Langer, *Tissue engineering: the design and fabrication of living replacement devices for surgical reconstruction and transplantation.* Lancet, 1999. **354 Suppl 1**: p. SI32-4.
4. Langer, R. and J.P. Vacanti, *Tissue engineering.* Science, 1993. **260**(5110): p. 920-6.
5. Leon, L. and H.P. Greisler, *Vascular grafts.* Expert Rev Cardiovasc Ther, 2003. **1**(4): p. 581-94.
6. Faries, P.L., et al., *A comparative study of alternative conduits for lower extremity revascularization: all-autogenous conduit versus prosthetic grafts.* J Vasc Surg, 2000. **32**(6): p. 1080-90.
7. Tiwari, A., et al., *Tissue engineering of vascular bypass grafts: role of endothelial cell extraction.* Eur J Vasc Endovasc Surg, 2001. **21**(3): p. 193-201.
8. Hirose, H., et al., *Coronary artery bypass grafting using the gastroepiploic artery in 1,000 patients.* Ann Thorac Surg, 2002. **73**(5): p. 1371-9.
9. Lehalle, B., et al., *Early rupture and degeneration of cryopreserved arterial allografts.* J Vasc Surg, 1997. **25**(4): p. 751-2.
10. Jackson, D.R. and D.W. Abel, *The homologous saphenous vein in arterial reconstruction.* Vasc Surg, 1972. **6**(2): p. 85-92.
11. Stephen, M., A.G. Sheil, and J. Wong, *Allograft vein arterial bypass.* Arch Surg, 1978. **113**(5): p. 591-3.
12. Dardik, H., et al., *Comparative decades of experience with glutaraldehyde-tanned human umbilical cord vein graft for lower limb revascularization: an analysis of 1275 cases.* J Vasc Surg, 2002. **35**(1): p. 64-71.
13. Speer, D.P., et al., *Biological effects of residual glutaraldehyde in glutaraldehyde-tanned collagen biomaterials.* J Biomed Mater Res, 1980. **14**(6): p. 753-64.
14. Kannan, R.Y., et al., *Current status of prosthetic bypass grafts: a review.* J Biomed Mater Res B Appl Biomater, 2005. **74**(1): p. 570-81.
15. Xue, L. and H.P. Greisler, *Biomaterials in the development and future of vascular grafts.* J Vasc Surg, 2003. **37**(2): p. 472-80.
16. Heilshorn, S.C., et al., *Endothelial cell adhesion to the fibronectin CS5 domain in artificial extracellular matrix proteins.* Biomaterials, 2003. **24**(23): p. 4245-52.
17. Prager, M., et al., *Collagen versus gelatin-coated Dacron versus stretch polytetrafluoroethylene in abdominal aortic bifurcation graft surgery: results of a seven-year prospective, randomized multicenter trial.* Surgery, 2001. **130**(3): p. 408-14.
18. Green, R.M., et al., *Prosthetic above-knee femoropopliteal bypass grafting: five-year results of a randomized trial.* J Vasc Surg, 2000. **31**(3): p. 417-25.
19. Chandy, T., et al., *Use of plasma glow for surface-engineering biomolecules to enhance bloodcompatibility of Dacron and PTFE vascular prosthesis.* Biomaterials, 2000. **21**(7): p. 699-712.

20. Friedman, S.G., et al., *A prospective randomized comparison of Dacron and polytetrafluoroethylene aortic bifurcation grafts.* Surgery, 1995. **117**(1): p. 7-10.
21. Ravi, S., Z. Qu, and E.L. Chaikof, *Polymeric materials for tissue engineering of arterial substitutes.* Vascular, 2009. **17 Suppl 1**: p. S45-54.
22. Buttafoco, L., et al., *Electrospinning of collagen and elastin for tissue engineering applications.* Biomaterials, 2006. **27**(5): p. 724-34.
23. Bank, A.J., et al., *Contribution of collagen, elastin, and smooth muscle to in vivo human brachial artery wall stress and elastic modulus.* Circulation, 1996. **94**(12): p. 3263-70.
24. Davis, G.E. and C.W. Camarillo, *An alpha 2 beta 1 integrin-dependent pinocytic mechanism involving intracellular vacuole formation and coalescence regulates capillary lumen and tube formation in three-dimensional collagen matrix.* Exp Cell Res, 1996. **224**(1): p. 39-51.
25. Reyes, C.D. and A.J. Garcia, *Alpha2beta1 integrin-specific collagen-mimetic surfaces supporting osteoblastic differentiation.* J Biomed Mater Res A, 2004. **69**(4): p. 591-600.
26. Knight, C.G., et al., *Identification in collagen type I of an integrin alpha2 beta1-binding site containing an essential GER sequence.* J Biol Chem, 1998. **273**(50): p. 33287-94.
27. Charulatha, V. and A. Rajaram, *Influence of different crosslinking treatments on the physical properties of collagen membranes.* Biomaterials, 2003. **24**(5): p. 759-67.
28. Seliktar, D., et al., *Dynamic mechanical conditioning of collagen-gel blood vessel constructs induces remodeling in vitro.* Ann Biomed Eng, 2000. **28**(4): p. 351-62.
29. Li, M., et al., *Electrospun protein fibers as matrices for tissue engineering.* Biomaterials, 2005. **26**(30): p. 5999-6008.
30. Cox, R.H., *Passive mechanics and connective tissue composition of canine arteries.* Am J Physiol, 1978. **234**(5): p. H533-41.
31. Silver, F.H., P.B. Snowhill, and D.J. Foran, *Mechanical behavior of vessel wall: a comparative study of aorta, vena cava, and carotid artery.* Ann Biomed Eng, 2003. **31**(7): p. 793-803.
32. Sherwood, L. *Human physiology : from cells to systems*. 2004; 5th:[1 v. (various pagings)].
33. Li, D.Y., et al., *Novel arterial pathology in mice and humans hemizygous for elastin.* J Clin Invest, 1998. **102**(10): p. 1783-7.
34. VanBavel, E., P. Siersma, and J.A. Spaan, *Elasticity of passive blood vessels: a new concept.* Am J Physiol Heart Circ Physiol, 2003. **285**(5): p. H1986-2000.
35. Sallach, R.E., *Recombinant elastin-mimetic protein polymer as design elements for an arterial substitute*, in *Bioengineering*. 2008, Georgia Institute of Technology: Atlanta, Georgia USA. p. 177.
36. Rucker, R.B. and M.A. Dubick, *Elastin metabolism and chemistry: potential roles in lung development and structure.* Environ Health Perspect, 1984. **55**: p. 179-91.
37. Petka, W.A., et al., *Reversible hydrogels from self-assembling artificial proteins.* Science, 1998. **281**(5375): p. 389-92.
38. Wright, E.R. and V.P. Conticello, *Self-assembly of block copolymers derived from elastin-mimetic polypeptide sequences.* Adv Drug Deliv Rev, 2002. **54**(8): p. 1057-73.
39. Urry, D.W., et al., *Temperature of polypeptide inverse temperature transition depends on mean residue hydrophobicity.* J Am Chem Soc, 1991. **113**: p. 4346-4348.
40. Bellingham, C.M., et al., *Recombinant human elastin polypeptides self-assemble into biomaterials with elastin-like properties.* Biopolymers, 2003. **70**(4): p. 445-55.
41. Sallach, R.E., et al., *Elastin-mimetic protein polymers capable of physical and chemical crosslinking.* Biomaterials, 2009. **30**(3): p. 409-22.

42. Keeley, F.W., C.M. Bellingham, and K.A. Woodhouse, *Elastin as a self-organizing biomaterial: use of recombinantly expressed human elastin polypeptides as a model for investigations of structure and self-assembly of elastin.* Philosophical Transactions of the Royal Society of London Series B-Biological Sciences, 2002. **357**(1418): p. 185-189.
43. Vieth, S., et al., *Microstructural and tensile properties of elastin-based polypeptides crosslinked with genipin and pyrroloquinoline quinone.* Biopolymers, 2007. **85**(3): p. 199-206.
44. Vrhovski, B. and A.S. Weiss, *Biochemistry of tropoelastin.* Eur J Biochem, 1998. **258**(1): p. 1-18.
45. Reiser, K., R.J. McCormick, and R.B. Rucker, *Enzymatic and nonenzymatic cross-linking of collagen and elastin.* FASEB J, 1992. **6**(7): p. 2439-49.
46. Eyre, D.R., M.A. Paz, and P.M. Gallop, *Cross-linking in collagen and elastin.* Annu Rev Biochem, 1984. **53**: p. 717-48.
47. Mansfield, P.B., A.R. Wechezak, and L.R. Sauvage, *Preventing thrombus on artifical vascular surfaces: true endothelial cell linings.* Trans Am Soc Artif Intern Organs, 1975. **21**: p. 264-72.
48. Herring, M., A. Gardner, and J. Glover, *A single-staged technique for seeding vascular grafts with autogenous endothelium.* Surgery, 1978. **84**(4): p. 498-504.
49. Herring, M.B., et al., *Seeding arterial prostheses with vascular endothelium. The nature of the lining.* Ann Surg, 1979. **190**(1): p. 84-90.
50. Deutsch, M., et al., *Clinical autologous in vitro endothelialization of infrainguinal ePTFE grafts in 100 patients: a 9-year experience.* Surgery, 1999. **126**(5): p. 847-55.
51. Salacinski, H.J., et al., *Cellular engineering of vascular bypass grafts: role of chemical coatings for enhancing endothelial cell attachment.* Med Biol Eng Comput, 2001. **39**(6): p. 609-18.
52. Rosenman, J.E., et al., *Kinetics of endothelial cell seeding.* J Vasc Surg, 1985. **2**(6): p. 778-84.
53. Bowlin, G.L., et al., *In vitro evaluation of electrostatic endothelial cell transplantation onto 4 mm interior diameter expanded polytetrafluoroethylene grafts.* J Vasc Surg, 1998. **27**(3): p. 504-11.
54. Aukhil, I., et al., *Cell- and heparin-binding domains of the hexabrachion arm identified by tenascin expression proteins.* J Biol Chem, 1993. **268**(4): p. 2542-53.
55. Hynes, R.O. and K.M. Yamada, *Fibronectins: multifunctional modular glycoproteins.* J Cell Biol, 1982. **95**(2 Pt 1): p. 369-77.
56. Kornblihtt, A.R., et al., *Primary structure of human fibronectin: differential splicing may generate at least 10 polypeptides from a single gene.* EMBO J, 1985. **4**(7): p. 1755-9.
57. Pearlstein, E., L.I. Gold, and A. Garcia-Pardo, *Fibronectin: a review of its structure and biological activity.* Mol Cell Biochem, 1980. **29**(2): p. 103-28.
58. Pearlstein, E., *Plasma membrane glycoprotein which mediates adhesion of fibroblasts to collagen.* Nature, 1976. **262**(5568): p. 497-500.
59. Leahy, D.J., I. Aukhil, and H.P. Erickson, *2.0 A crystal structure of a four-domain segment of human fibronectin encompassing the RGD loop and synergy region.* Cell, 1996. **84**(1): p. 155-64.
60. Aota, S., M. Nomizu, and K.M. Yamada, *The short amino acid sequence Pro-His-Ser-Arg-Asn in human fibronectin enhances cell-adhesive function.* J Biol Chem, 1994. **269**(40): p. 24756-61.

61. Petrie, T.A., et al., *Integrin specificity and enhanced cellular activities associated with surfaces presenting a recombinant fibronectin fragment compared to RGD supports.* Biomaterials, 2006. **27**(31): p. 5459-70.
62. Ruoslahti, E. and M.D. Pierschbacher, *New perspectives in cell adhesion: RGD and integrins.* Science, 1987. **238**(4826): p. 491-7.
63. Macarak, E.J. and P.S. Howard, *Adhesion of endothelial cells to extracellular matrix proteins.* J Cell Physiol, 1983. **116**(1): p. 76-86.
64. Kaufmann, D., et al., *Chemical conjugation of linear and cyclic RGD moieties to a recombinant elastin-mimetic polypeptide--a versatile approach towards bioactive protein hydrogels.* Macromol Biosci, 2008. **8**(6): p. 577-88.
65. Pierschbacher, M.D. and E. Ruoslahti, *Cell attachment activity of fibronectin can be duplicated by small synthetic fragments of the molecule.* Nature, 1984. **309**(5963): p. 30-3.
66. Pierschbacher, M.D. and E. Ruoslahti, *Variants of the cell recognition site of fibronectin that retain attachment-promoting activity.* Proc Natl Acad Sci U S A, 1984. **81**(19): p. 5985-8.
67. Pollard, T.D. and W.C. Earnshaw, *Cell biology*. 2002, Philadelphia: Saunders. xiv, 805 p.
68. Miranti, C.K. and J.S. Brugge, *Sensing the environment: a historical perspective on integrin signal transduction.* Nat Cell Biol, 2002. **4**(4): p. E83-90.
69. Arnaout, M.A., B. Mahalingam, and J.P. Xiong, *Integrin structure, allostery, and bidirectional signaling.* Annu Rev Cell Dev Biol, 2005. **21**: p. 381-410.
70. Reyes, C.D., T.A. Petrie, and A.J. Garcia, *Mixed extracellular matrix ligands synergistically modulate integrin adhesion and signaling.* J Cell Physiol, 2008. **217**(2): p. 450-8.
71. Horton, M.A., *The alpha v beta 3 integrin "vitronectin receptor".* Int J Biochem Cell Biol, 1997. **29**(5): p. 721-5.
72. Dormond, O., et al., *Prostaglandin E2 promotes integrin alpha Vbeta 3-dependent endothelial cell adhesion, rac-activation, and spreading through cAMP/PKA-dependent signaling.* J Biol Chem, 2002. **277**(48): p. 45838-46.
73. Romer, L.H., K.G. Birukov, and J.G. Garcia, *Focal adhesions: paradigm for a signaling nexus.* Circ Res, 2006. **98**(5): p. 606-16.
74. Zamir, E. and B. Geiger, *Molecular complexity and dynamics of cell-matrix adhesions.* J Cell Sci, 2001. **114**(Pt 20): p. 3583-90.
75. Geiger, B., et al., *Transmembrane crosstalk between the extracellular matrix--cytoskeleton crosstalk.* Nat Rev Mol Cell Biol, 2001. **2**(11): p. 793-805.
76. Ponti, A., et al., *Two distinct actin networks drive the protrusion of migrating cells.* Science, 2004. **305**(5691): p. 1782-6.
77. Alberts, B., *Molecular biology of the cell*. 4th ed. 2002, New York: Garland Science. xxxiv, [1548] p.
78. Lauffenburger, D.A. and A.F. Horwitz, *Cell migration: a physically integrated molecular process.* Cell, 1996. **84**(3): p. 359-69.
79. Stegemann, J.P. and R.M. Nerem, *Phenotype modulation in vascular tissue engineering using biochemical and mechanical stimulation.* Ann Biomed Eng, 2003. **31**(4): p. 391-402.
80. Mandal, B.B. and S.C. Kundu, *Cell proliferation and migration in silk fibroin 3D scaffolds.* Biomaterials, 2009. **30**(15): p. 2956-65.
81. Richardson, T.P., et al., *Polymeric system for dual growth factor delivery.* Nat Biotechnol, 2001. **19**(11): p. 1029-34.

82. Khademhosseini, A., et al., *Microscale technologies for tissue engineering and biology.* Proc Natl Acad Sci U S A, 2006. **103**(8): p. 2480-7.
83. Kaufmann, D. and R. Weberskirch, *Efficient synthesis of protein-drug conjugates using a functionalizable recombinant elastin-mimetic polypeptide.* Macromol Biosci, 2006. **6**(11): p. 952-8.
84. Marampon, F., et al., *Nerve Growth factor regulation of cyclin D1 in PC12 cells through a p21RAS extracellular signal-regulated kinase pathway requires cooperative interactions between Sp1 and nuclear factor-kappaB.* Mol Biol Cell, 2008. **19**(6): p. 2566-78.
85. Kapur, T.A. and M.S. Shoichet, *Chemically-bound nerve growth factor for neural tissue engineering applications.* J Biomater Sci Polym Ed, 2003. **14**(4): p. 383-94.
86. Cao, X. and M.S. Shoichet, *Defining the concentration gradient of nerve growth factor for guided neurite outgrowth.* Neuroscience, 2001. **103**(3): p. 831-40.
87. Massia, S.P. and J.A. Hubbell, *Covalent surface immobilization of Arg-Gly-Asp- and Tyr-Ile-Gly-Ser-Arg-containing peptides to obtain well-defined cell-adhesive substrates.* Anal Biochem, 1990. **187**(2): p. 292-301.
88. Grinnell, F., *Focal adhesion sites and the removal of substratum-bound fibronectin.* J Cell Biol, 1986. **103**(6 Pt 2): p. 2697-706.
89. Niveleau, A., et al., *Grafting peptides onto polystyrene microplates for ELISA.* J Immunol Methods, 1995. **182**(2): p. 227-34.
90. Wang, H., et al., *Modulating cell adhesion and spreading by control of FnIII7-10 orientation on charged self-assembled monolayers (SAMs) of alkanethiolates.* J Biomed Mater Res A, 2006. **77**(4): p. 672-8.
91. Petrie, T.A., et al., *The effect of integrin-specific bioactive coatings on tissue healing and implant osseointegration.* Biomaterials, 2008. **29**(19): p. 2849-57.
92. Welsh, E.R. and D.A. Tirrell, *Engineering the extracellular matrix: a novel approach to polymeric biomaterials. I. Control of the physical properties of artificial protein matrices designed to support adhesion of vascular endothelial cells.* Biomacromolecules, 2000. **1**(1): p. 23-30.
93. Liu, J.C. and D.A. Tirrell, *Cell response to RGD density in cross-linked artificial extracellular matrix protein films.* Biomacromolecules, 2008. **9**(11): p. 2984-8.
94. Panitch, A., et al., *Design and Biosynthesis of Elastin-like Artificial Extracellular Matrix Proteins Containing Periodically Spaced Fibronectin CS5 Domains.* Macromolecules, 1999. **32**(5): p. 1701-1703.
95. Ji, T.H., *Bifunctional reagents.* Methods Enzymol, 1983. **91**: p. 580-609.
96. Wong, S.S. and L.J. Wong, *Chemical crosslinking and the stabilization of proteins and enzymes.* Enzyme Microb Technol, 1992. **14**(11): p. 866-74.
97. Cutler, S.M., *Engineering cell adhesive surfaces that support integrin alpha-5-beta-1 binding using a recombinant fragment of fibronectin*, in *Biomedical Engineering*. 2002, Georgia Institute of Technology: Atlanta, Georgia USA. p. 61.
98. Liang, H.C., et al., *Crosslinking structures of gelatin hydrogels crosslinked with genipin or a water-soluble carbodiimide.* J Appl Polym Sci, 2004. **91**: p. 4017-4026.
99. Butler, M.F., Y.F. Ng, and P.D.A. Pudney, *Mechanism and kinetics of the crosslinking reaction between biopolymers containing primary amine groups and genipin.* Journal of Polymer Science Part a-Polymer Chemistry, 2003. **41**(24): p. 3941-3953.
100. Mi, F.L., et al., *In vitro evaluation of a chitosan membrane cross-linked with genipin.* J Biomater Sci Polym Ed, 2001. **12**(8): p. 835-50.
101. Chow, D.C., et al., *Ultra-high expression of a thermally responsive recombinant fusion protein in E-coli.* Biotechnology Progress, 2006. **22**(3): p. 638-646.

102. Katayama, M., et al., *Isolation and characterization of two monoclonal antibodies that recognize remote epitopes on the cell-binding domain of human fibronectin.* Exp Cell Res, 1989. **185**(1): p. 229-36.
103. Connolly, J.M., et al., *Triglycidylamine crosslinking of porcine aortic valve cusps or bovine pericardium results in improved biocompatibility, biomechanics, and calcification resistance: chemical and biological mechanisms.* Am J Pathol, 2005. **166**(1): p. 1-13.
104. Fall, R.R. and P.R. Vagelos, *Acetyl coenzyme A carboxylase. Proteolytic modification of biotin carboxyl carrier protein.* J Biol Chem, 1973. **248**(6): p. 2078-88.
105. Schoen, R.C., K.L. Bentley, and R.J. Klebe, *Monoclonal antibody against human fibronectin which inhibits cell attachment.* Hybridoma, 1982. **1**(2): p. 99-108.
106. Keselowsky, B.G., D.M. Collard, and A.J. Garcia, *Surface chemistry modulates fibronectin conformation and directs integrin binding and specificity to control cell adhesion.* J Biomed Mater Res A, 2003. **66**(2): p. 247-59.
107. Lightner, V.A. and H.P. Erickson, *Binding of hexabrachion (tenascin) to the extracellular matrix and substratum and its effect on cell adhesion.* J Cell Sci, 1990. **95 (Pt 2)**: p. 263-77.
108. Cutler, S.M. and A.J. Garcia, *Engineering cell adhesive surfaces that direct integrin alpha5beta1 binding using a recombinant fragment of fibronectin.* Biomaterials, 2003. **24**(10): p. 1759-70.
109. Grant, R.P., et al., *Structural requirements for biological activity of the ninth and tenth FIII domains of human fibronectin.* J Biol Chem, 1997. **272**(10): p. 6159-66.
110. Cronan, J.E., Jr., *Biotination of proteins in vivo. A post-translational modification to label, purify, and study proteins.* J Biol Chem, 1990. **265**(18): p. 10327-33.
111. McDevitt, T.C., K.E. Nelson, and P.S. Stayton, *Constrained cell recognition peptides engineered into streptavidin.* Biotechnol Prog, 1999. **15**(3): p. 391-6.
112. Bix, G., et al., *Endorepellin causes endothelial cell disassembly of actin cytoskeleton and focal adhesions through alpha2beta1 integrin.* J Cell Biol, 2004. **166**(1): p. 97-109.
113. Senior, R.M., et al., *Val-Gly-Val-Ala-Pro-Gly, a repeating peptide in elastin, is chemotactic for fibroblasts and monocytes.* J Cell Biol, 1984. **99**(3): p. 870-4.
114. Daamen, W.F., et al., *Elastin as a biomaterial for tissue engineering.* Biomaterials, 2007. **28**(30): p. 4378-98.
115. Nicol, A., D.C. Gowda, and D.W. Urry, *Cell adhesion and growth on synthetic elastomeric matrices containing Arg-Gly-Asp-Ser-3.* J Biomed Mater Res, 1992. **26**(3): p. 393-413.
116. Freij-Larsson, C., et al., *Adsorption behaviour of amphiphilic polymers at hydrophobic surfaces: effects on protein adsorption.* Biomaterials, 1996. **17**(22): p. 2199-207.
117. Curtis, A.S. and J.V. Forrester, *The competitive effects of serum proteins on cell adhesion.* J Cell Sci, 1984. **71**: p. 17-35.
118. Zhang, Y., et al., *Fibronectin immobilized by covalent conjugation or physical adsorption shows different bioactivity on aminated-PET.* Materials Science and Engineering: C, 2007. **27**(2): p. 213-219.